arXiv:1711.03077
*To be published in **Physical Review B***

Surface impedance and optimum surface resistance of a superconductor with imperfect surface

Alex Gurevich[1,*] and Takayuki Kubo[1,2,3,†]

[1] *Department of Physics and Center for Accelerator Science, Old Dominion University, Norfolk, Virginia 23529, USA.*
[2] *KEK (High Energy Accelerator Research Organization), Tsukuba, Ibaraki 305-0801, Japan.*
[3] *SOKENDAI (the Graduate University for Advanced Studies), Hayama, Kanagawa 240-0115, Japan.*

The work of A.G. was supported by NSF under Grant PHY-1416051. The work of T.K. was supported by Japan society for the promotion of science (JSPS) Grant-in-Aid for Young Scientists (A) #17H04839 and JSPS Grant-in-Aid for Challenging Exploratory Research, #26600142.

The surface resistance of an SRF cavity is usually written as the summation of

R_{MB} : Mattis-Bardeen surface resistance

The surface resistance of an SRF cavity is usually written as the summation of

R_{MB} : Mattis-Bardeen surface resistance

R_{flux} : trapped flux contribution

The surface resistance of an SRF cavity is usually written as the summation of

R_{MB} : Mattis-Bardeen surface resistance

R_{others} : others

Damaged layer

Metallic sub-oxide

Subgap states

Dielectric losses

etc

R_{flux} : trapped flux contribution

The surface resistance of an SRF cavity is usually written as the summation of

R_{MB}

R_{others}

- Damaged layer
- Metallic sub-oxide
- Subgap states
- Dielectric losses
- etc

R_{flux}

$$R_s = R_{MB} + R_{flux} + R_{others}$$

Today, R_{flux} can be substantially reduced by cooling down a cavity with a large temperature gradient.

- A. Romanenko, et al., Appl. Phys. Lett. **105**, 234103 (2014).
- S. Posen et al., J. Appl. Phys. **119**, 213903 (2016)
- S. Huang, T. Kubo, and R. Geng, Phys. Rev. Accel. Beams **19**, 082001 (2016)

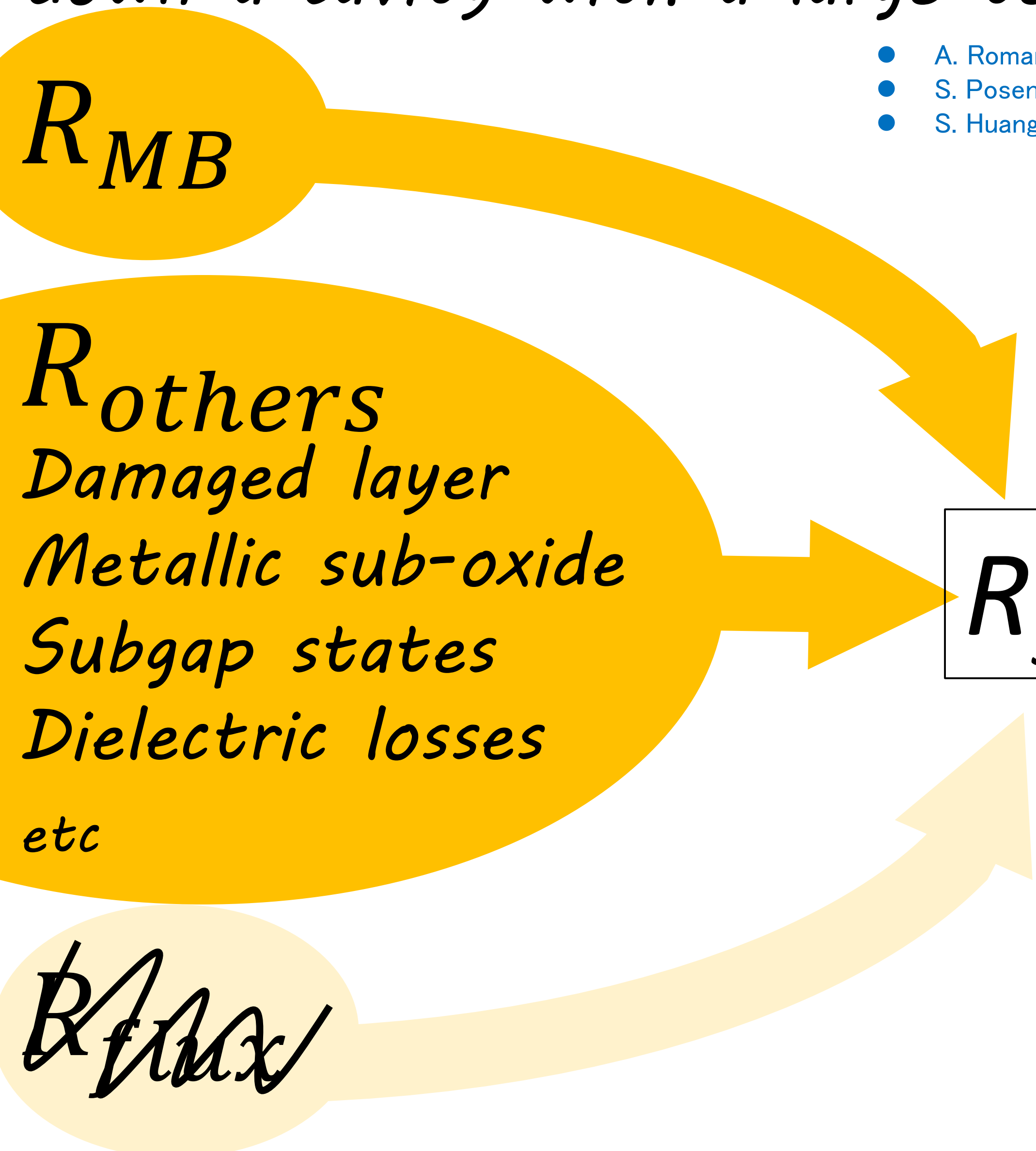

$$R_s = R_{MB} + R_{flux} + R_{others}$$

Today, R_{flux} can be substantially reduced by cooling down a cavity with a large temperature gradient.

- A. Romanenko, et al., Appl. Phys. Lett. **105**, 234103 (2014).
- S. Posen et al., J. Appl. Phys. **119**, 213903 (2016)
- S. Huang, T. Kubo, and R. Geng, Phys. Rev. Accel. Beams **19**, 082001 (2016)

R_{MB}

R_{others}

Damaged layer

Metallic sub-oxide

Subgap states

Dielectric losses

etc

$\cancel{R_{flux}}$

$$R_s = R_{MB} + \cancel{R_{flux}} + R_{others}$$

Understanding this part is becoming important more and more!

Today, *R_{flux} can be substantially reduced* by cooling down a cavity with a large temperature gradient.

- A. Romanenko, et al., Appl. Phys. Lett. **105**, 234103 (2014).
- S. Posen et al., J. Appl. Phys. **119**, 213903 (2016)
- S. Huang, T. Kubo, and R. Geng, Phys. Rev. Accel. Beams **19**, 082001 (2016)

R_{MB}

R_{others}

Damaged layer

Metallic sub-oxide

Subgap states

Dielectric losses

etc

~~R_{flux}~~

$R_s = R_{MB}$ ~~$+ R_{flux}$~~ $+ R_{others}$

Would contain information on the meaning of surface processing recipes.

Based on the BCS theory we calculate Rs simultaneously taking into account both the contributions.

R_{MB}

R_{others}

Damaged layer

Metallic sub-oxide

Subgap states

Dielectric losses

etc

R_{flux}

$$R_s = R_{MB} + R_{flux} + R_{others}$$

Structures, parameters, and theoretical tool

superconductors with imperfect surface

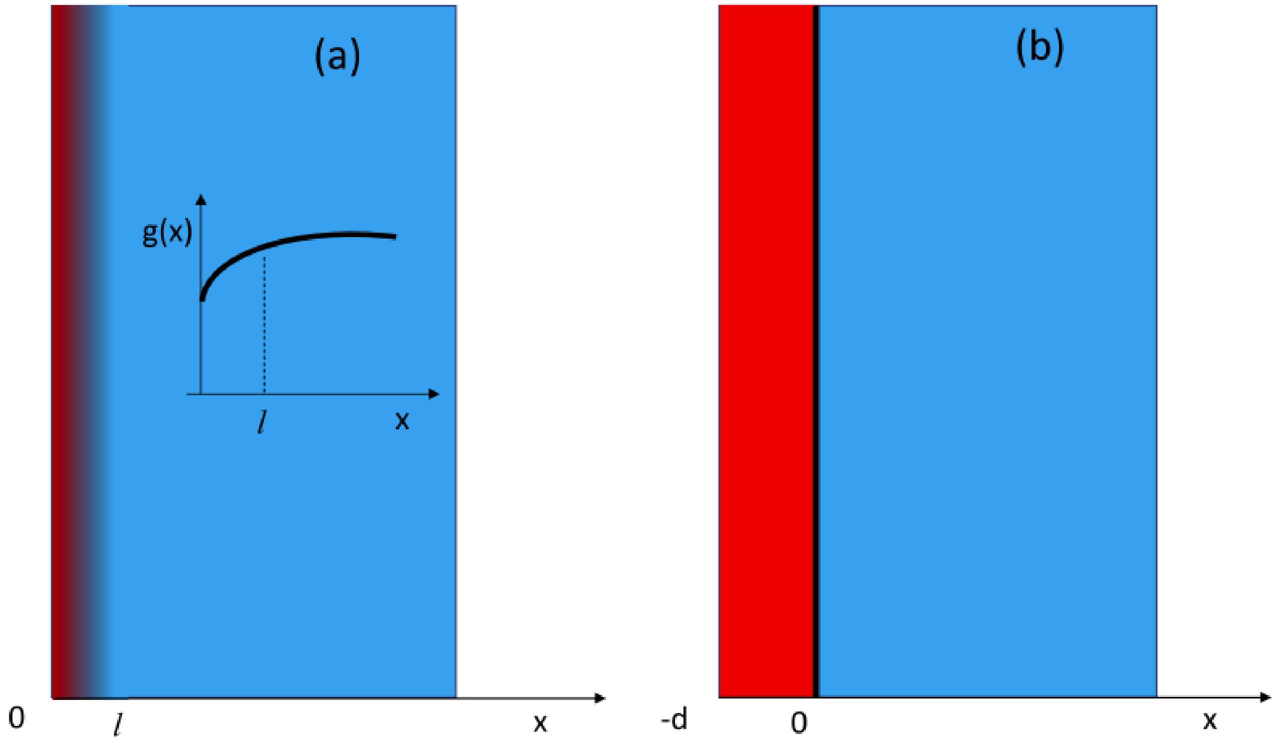

FIG. 1. (a) A surface layer of gradually reduced BCS pairing constant $g(x)$. Inset shows a profile of $g(x)$. (b) A superconductor covered with a normal layer of thickness d. The vertical black line in (b) shows the S-N interface giving rise to the contact resistance R_B.

superconductors with imperfect surface

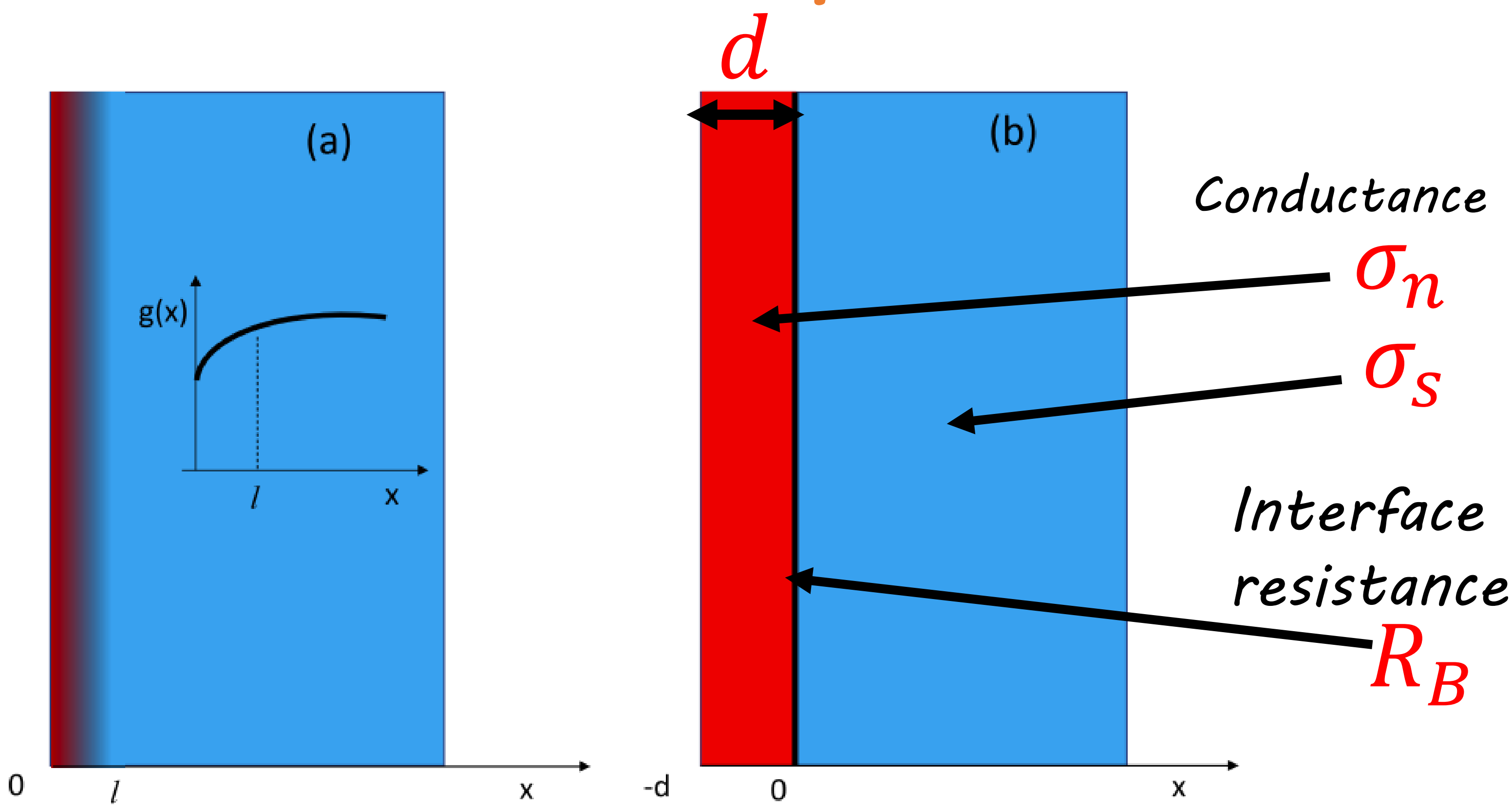

FIG. 1. (a) A surface layer of gradually reduced BCS pairing constant $g(x)$. Inset shows a profile of $g(x)$. (b) A superconductor covered with a normal layer of thickness d. The vertical black line in (b) shows the S-N interface giving rise to the contact resistance R_B.

superconductors with imperfect surface

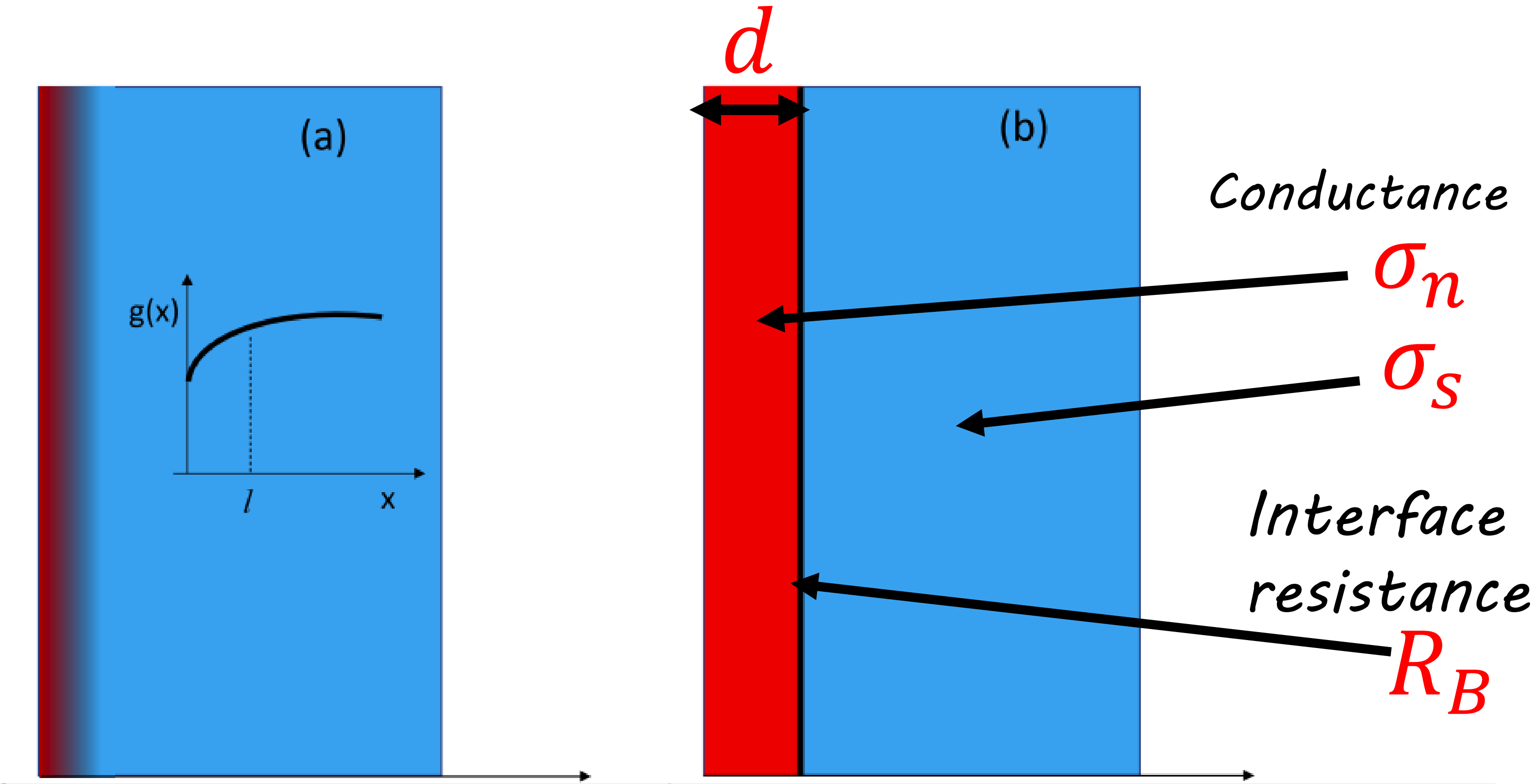

These structures model realistic surfaces of superconducting materials which can contain **oxide layers, absorbed impurities or nonstoichiometric composition**.

Theoretical tool

We use the quasiclassical theory in the diffusive limit.

- **Usadel equation** $$\xi_j^2\theta'' = -\frac{\Delta}{\Delta_\infty}\cos\theta + \frac{\hbar\omega_n}{\Delta_\infty}\sin\theta \qquad \xi_j \equiv \sqrt{\hbar D_j/2\Delta_\infty}\ (j = \mathrm{N, S})$$
- **Self-consistency condition** $$\Delta(x) = 2\pi k_B T g(x)\sum_{\omega_n}^{\Omega}\sin\theta(x)$$
- **Boundary conditions** $$\theta'|_{\mathrm{surface}} = 0, \qquad \sigma_n R_B \theta'_- = \sin(\theta_0 - \theta_-)$$ $$\theta(\infty) = \theta_\infty, \qquad \sigma_n\theta'_- = \sigma_s\theta'_0,$$

K. D. Usadel, Phys. Rev. Lett. **25**, 507 (1970).
M. Yu. Kuprianov and V. F. Lukichev, Sov. Phys. JETP **67**, 1163 (1988).

It is convenient to define the following dimensionless parameters:

$$\alpha = \frac{N_n}{N_s}\frac{d}{\xi_S} \qquad \beta = \frac{4e^2}{\hbar}R_B N_n \Delta d,$$

Theoretical tool

We use the quasiclassical theory in the diffusive limit.

- **Usadel equation** $\xi_j^2 \theta'' = -\frac{\Delta}{\Delta_\infty}\cos\theta + \frac{\hbar\omega_n}{\Delta_\infty}\sin\theta$ $\quad \xi_j \equiv \sqrt{\hbar D_j / 2\Delta_\infty}\ (j = \mathrm{N, S})$
- **Self-consistency condition** $\Delta(x) = 2\pi k_B T g(x) \sum_{\omega_n}^{\Omega} \sin\theta(x)$
- **Boundary conditions** $\theta'|_{\mathrm{surface}} = 0, \quad \sigma_n R_B \theta'_- = \sin(\theta_0 - \theta_-)$
  $\theta(\infty) = \theta_\infty, \quad \sigma_n \theta'_- = \sigma_s \theta'_0,$

K. D. Usadel, Phys. Rev. Lett. **25**, 507 (1970).
M. Yu. Kuprianov and V. F. Lukichev, Sov. Phys. JETP **67**, 1163 (1988).

It is convenient to define the following dimensionless parameters:

$$\alpha = \frac{N_n}{N_s}\frac{d}{\xi_S} \qquad \beta = \frac{4e^2}{\hbar} R_B N_n \Delta d,$$

$$\alpha = \frac{N_n}{N_s}\frac{d}{\xi_s} = 0.05$$

(when d = 1nm, ξ_s = 20nm, and $N_n = N_s$)

Theoretical tool

We use the quasiclassical theory in the diffusive limit.

- **Usadel equation** $$\xi_j^2\theta'' = -\frac{\Delta}{\Delta_\infty}\cos\theta + \frac{\hbar\omega_n}{\Delta_\infty}\sin\theta \qquad \xi_j \equiv \sqrt{\hbar D_j/2\Delta_\infty}\ (j = \mathrm{N, S})$$
- **Self-consistency condition** $$\Delta(x) = 2\pi k_B T g(x)\sum_{\omega_n}^{\Omega}\sin\theta(x)$$
- **Boundary conditions** $$\theta'|_{\mathrm{surface}} = 0, \qquad \sigma_n R_B \theta'_- = \sin(\theta_0 - \theta_-)$$ $$\theta(\infty) = \theta_\infty, \qquad \sigma_n\theta'_- = \sigma_s\theta'_0,$$

K. D. Usadel, Phys. Rev. Lett. **25**, 507 (1970).
M. Yu. Kuprianov and V. F. Lukichev, Sov. Phys. JETP **67**, 1163 (1988).

It is convenient to define the following dimensionless parameters:

$$\alpha = \frac{N_n}{N_s}\frac{d}{\xi_S} \qquad \beta = \frac{4e^2}{\hbar}R_B N_n \Delta d,$$

$$\alpha = \frac{N_n}{N_s}\frac{d}{\xi_s} = 0.05$$ (when d = 1nm, ξ_s = 20nm, and $N_n = N_s$)

$$\beta = \frac{4e^2}{\hbar}R_B N_n \Delta d = \frac{16d}{\xi_0}\frac{R_B}{R_K\lambda_F^2} \sim \frac{R_B}{10^{-14}\Omega\mathrm{m}^2}$$ (when d = 1nm, ξ_0 = 40nm)

For example, R_B of YBCO/Ag obtained in [J. W. Ekin et al., Appl. Phys. Lett. **62**, 369 (1993)] is $R_B \sim 10^{-13}$-$10^{-12}\Omega$m2, which yields β~10-100.

Theoretical tool

We use the quasiclassical theory in the diffusive limit.

- Usadel equation $\xi_j^2\theta'' = -\frac{\Delta}{\Delta_\infty}\cos\theta + \frac{\hbar\omega_n}{\Delta_\infty}\sin\theta$ $\quad \xi_j \equiv \sqrt{\hbar D_j/2\Delta_\infty}\ (j = \mathrm{N, S})$
- Self-consistency condition $\Delta(x) = 2\pi k_B T g(x)\sum_{\omega_n}^{\Omega}\sin\theta(x)$
- Boundary conditions $\theta'|_{\mathrm{surface}} = 0, \quad \sigma_n R_B\theta'_- = \sin(\theta_0 - \theta_-)$ $\quad \theta(\infty) = \theta_\infty, \quad \sigma_n\theta'_- = \sigma_s\theta'_0,$

K. D. Usadel, Phys. Rev. Lett. **25**, 507 (1970).
M. Yu. Kuprianov and V. F. Lukichev, Sov. Phys. JETP **67**, 1163 (1988).

It is convenient to define the following dimensionless parameters:

$$\alpha = \frac{N_n}{N_s}\frac{d}{\xi_S} \qquad \beta = \frac{4e^2}{\hbar}R_B N_n\Delta d,$$

➡ Normal and anomalous Quasiclassical Matsubara Green functions

T. Matsubara, Prog. Theor. Phys. **14**, 351 (1955).

$$G = \cos\theta \qquad F = \sin\theta$$

➡ Penetration depth

Theoretical tool

We use the quasiclassical theory in the diffusive limit.

- Usadel equation $\xi_j^2\theta'' = -\frac{\Delta}{\Delta_\infty}\cos\theta + \frac{\hbar\omega_n}{\Delta_\infty}\sin\theta$ $\quad \xi_j \equiv \sqrt{\hbar D_j/2\Delta_\infty}\ (j = \mathrm{N, S})$
- Self-consistency condition $\Delta(x) = 2\pi k_B T g(x)\sum_{\omega_n}^{\Omega}\sin\theta(x)$
- Boundary conditions $\theta'|_{\mathrm{surface}} = 0, \quad \sigma_n R_B\theta'_- = \sin(\theta_0 - \theta_-)$, $\quad \theta(\infty) = \theta_\infty, \quad \sigma_n\theta'_- = \sigma_s\theta'_0,$

K. D. Usadel, Phys. Rev. Lett. **25**, 507 (1970).
M. Yu. Kuprianov and V. F. Lukichev, Sov. Phys. JETP **67**, 1163 (1988).

It is convenient to define the following dimensionless parameters:

$$\alpha = \frac{N_n}{N_s}\frac{d}{\xi_S} \qquad \beta = \frac{4e^2}{\hbar}R_B N_n \Delta d,$$

➡ Normal and anomalous Quasiclassical Matsubara Green functions

T. Matsubara, Prog. Theor. Phys. **14**, 351 (1955).

$$G = \cos\theta \qquad F = \sin\theta$$

➡ Penetration depth

➡ Retarded normal and anomalous Quasiclassical Green functions

$$G^R = \cosh\theta \qquad F^R = \sinh\theta$$

➡ Density of states and surface resistance

Density of States

Density of states

DOS of Normal conductor

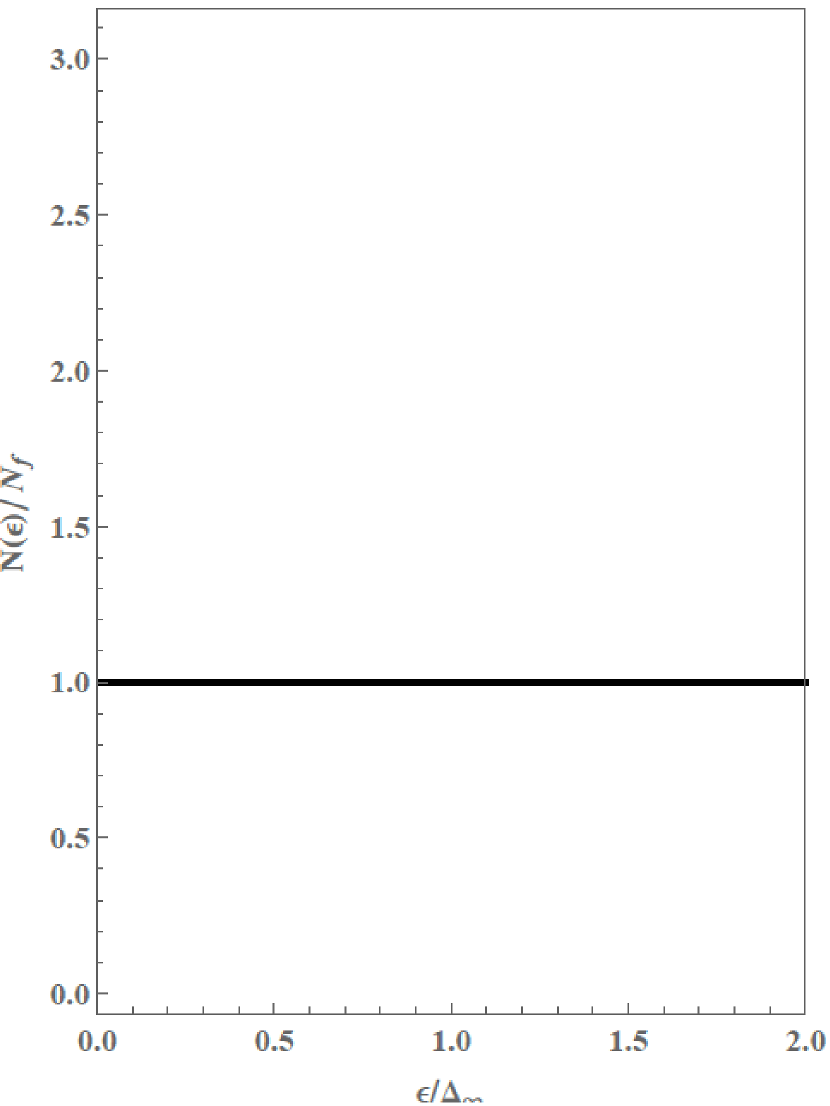

Density of states

DOS of Normal conductor

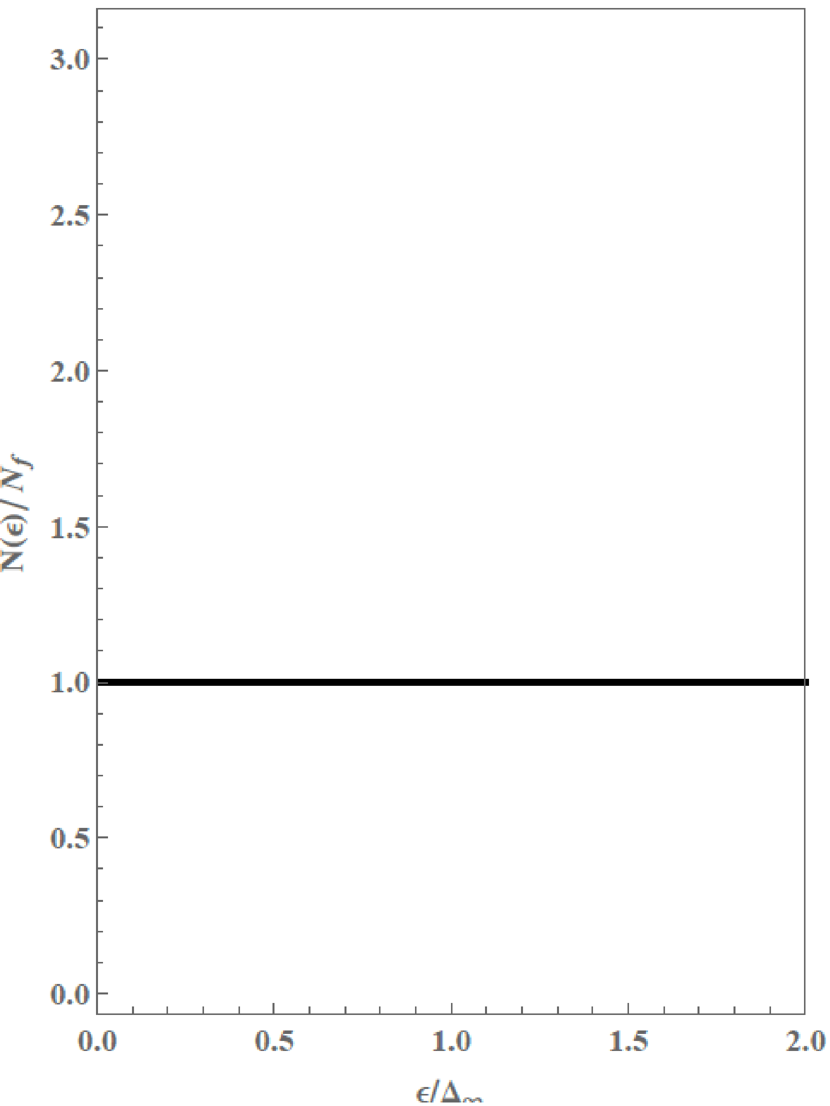

DOS of BCS superconductor

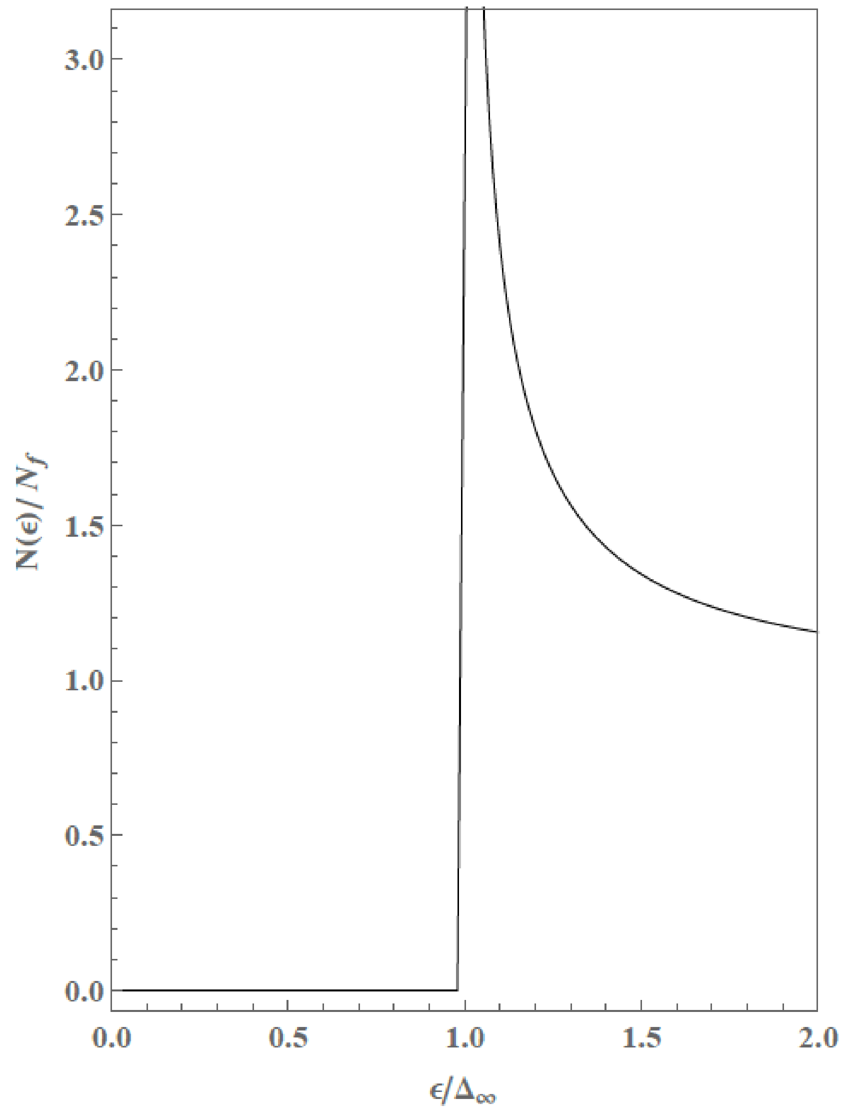

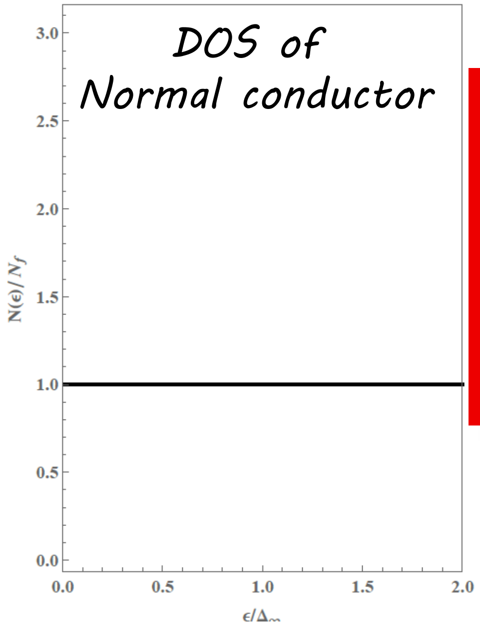

Normal conductor

BCS superconductor

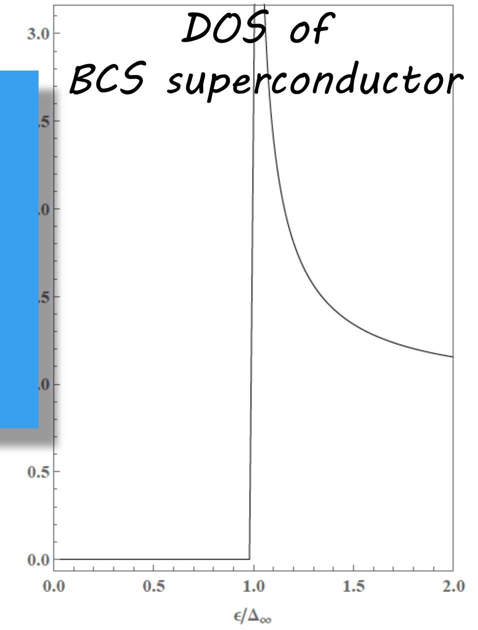

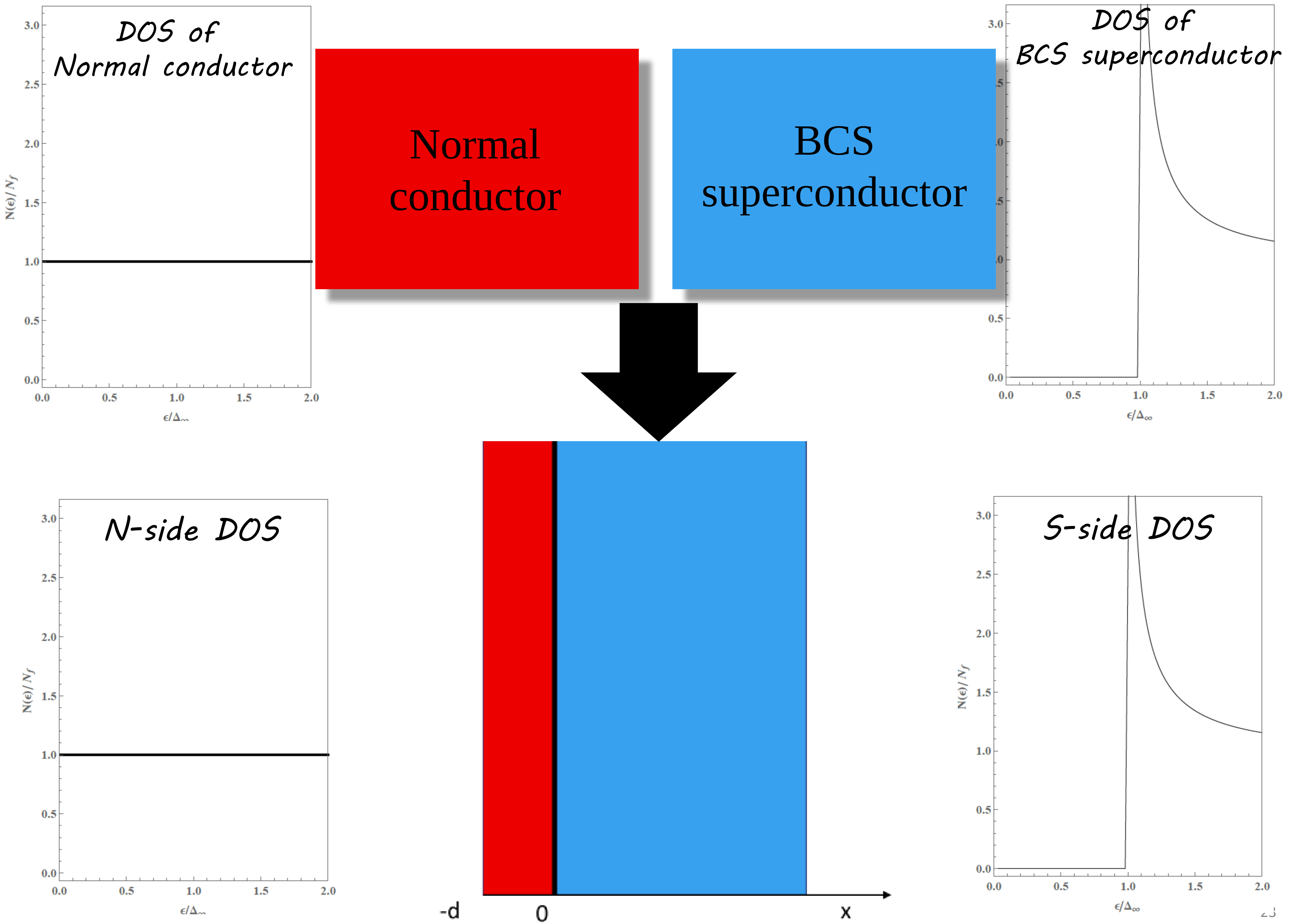
DOS of
Normal conductor
Normal
conductor
BCS
superconductor
DOS of
BCS superconductor
N-side DOS
S-side DOS
N(ϵ)/N_f
ϵ/Δ∞
-d
0
x

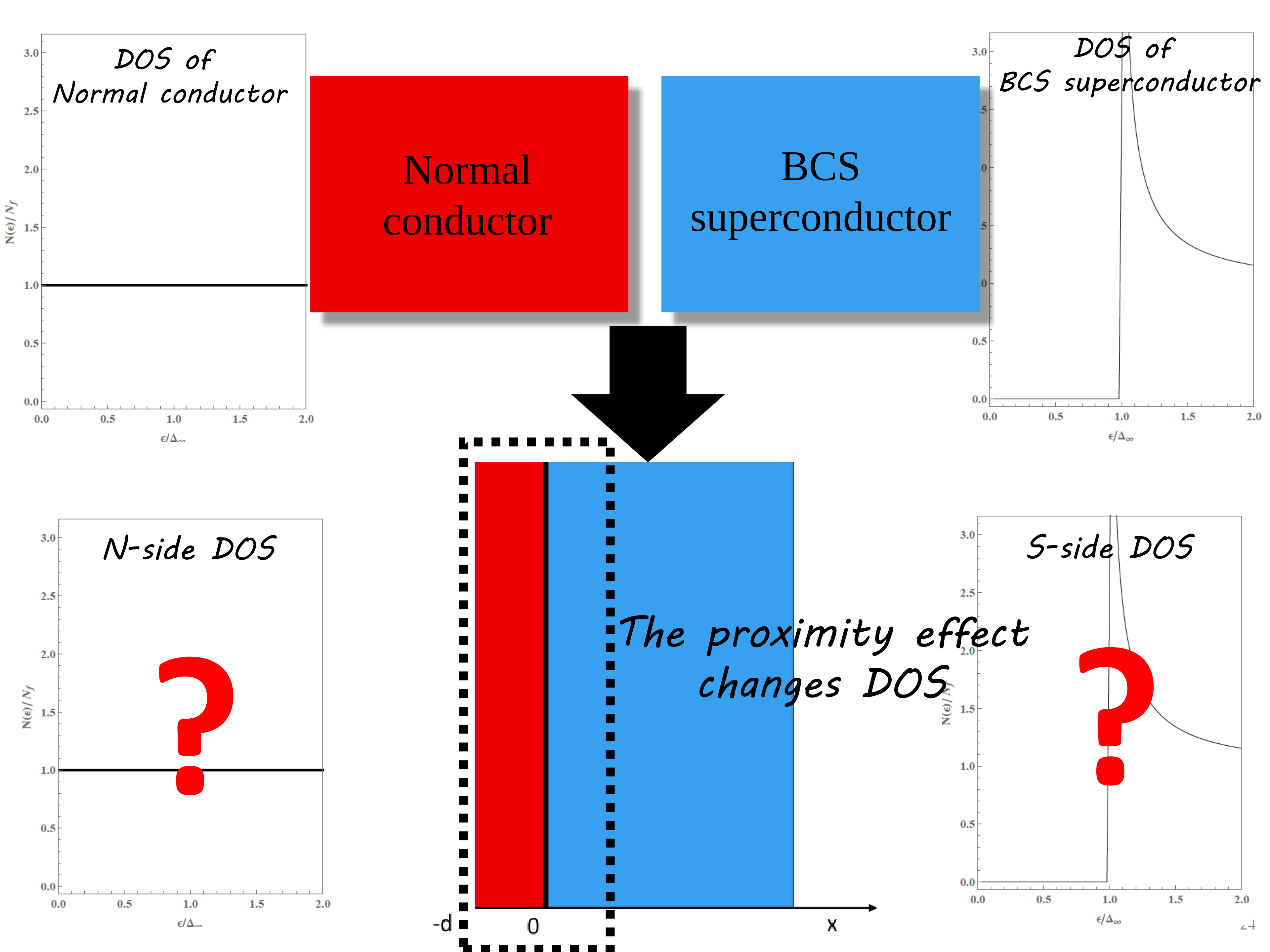
DOS of
Normal conductor
Normal conductor
BCS superconductor
DOS of
BCS superconductor
N-side DOS
S-side DOS
?
?
The proximity effect
changes DOS
-d
0
x
N(ε)/N_f
ε/Δ∞
0.0
0.5
1.0
1.5
2.0
2.5
3.0

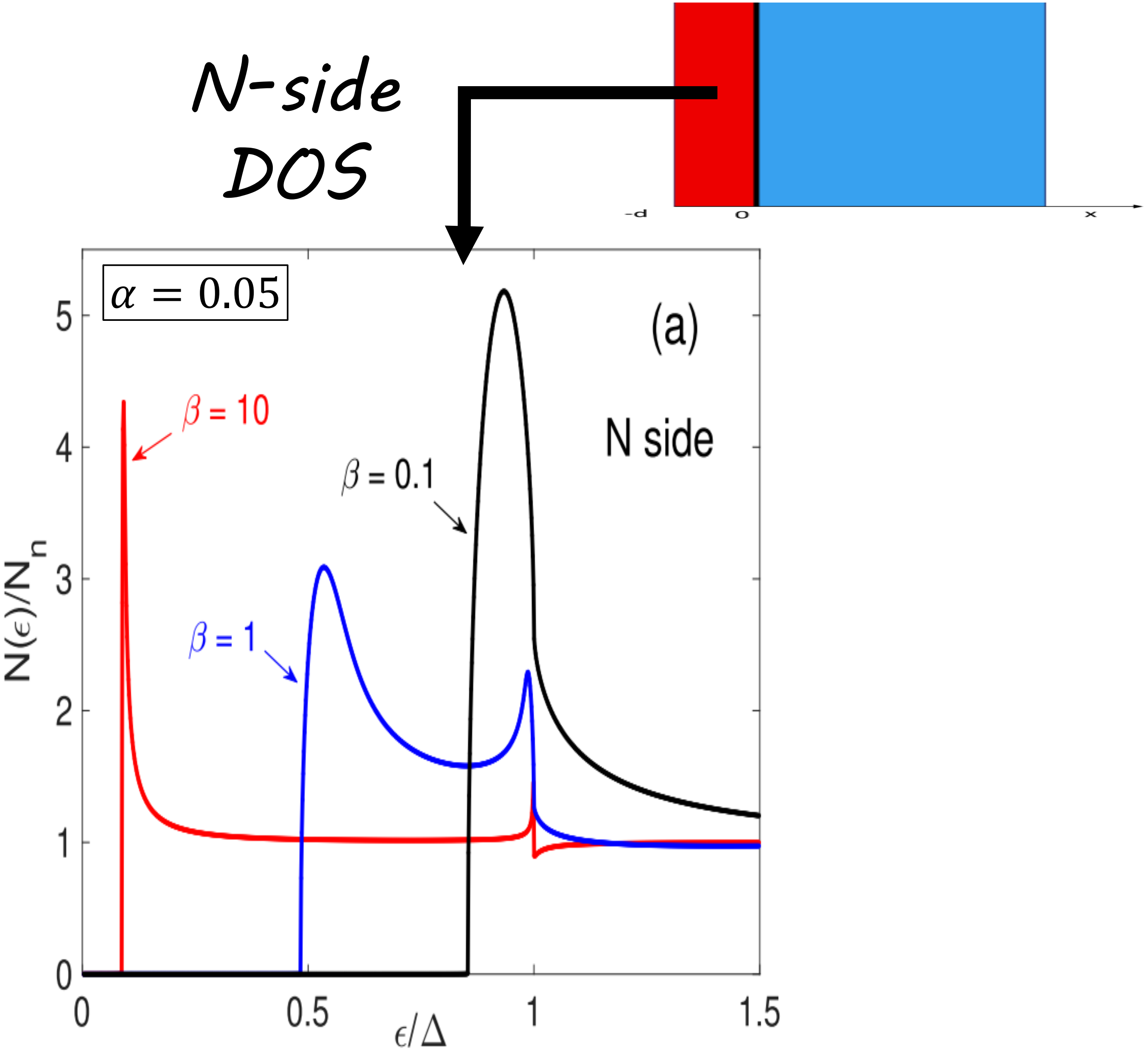

$$\beta = \frac{4e^2}{\hbar} R_B N_n \Delta d,$$

N-side DOS

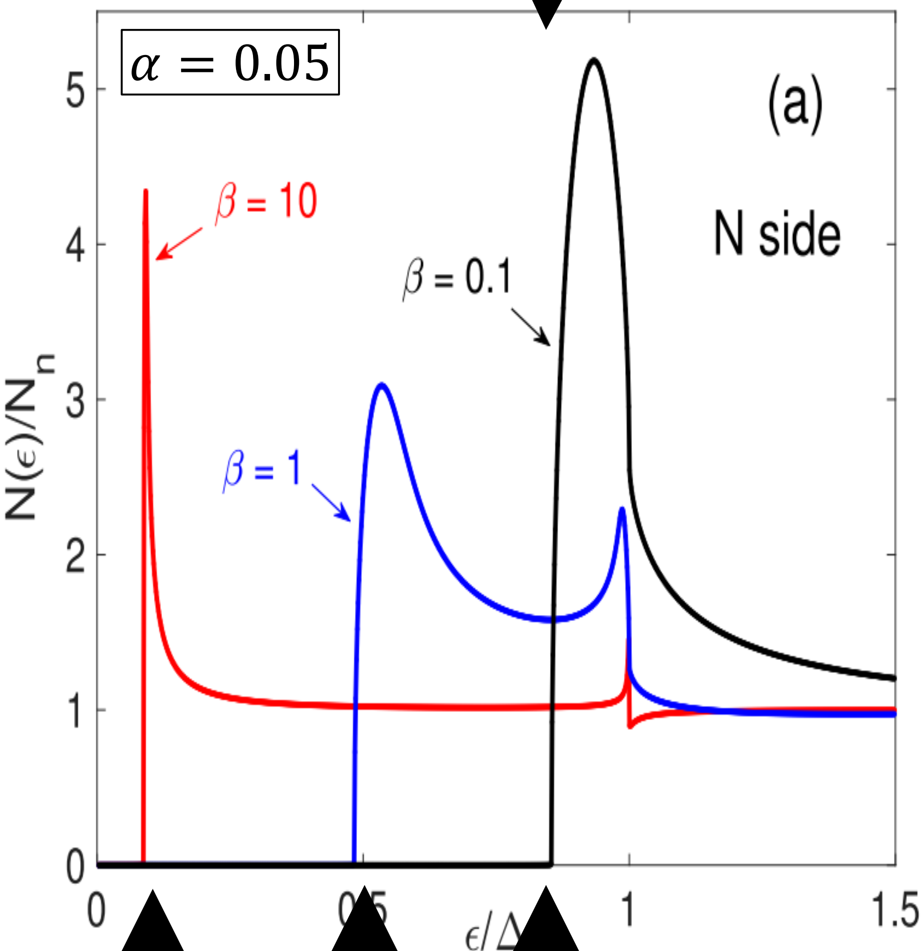

minigap

$$\beta = \frac{4e^2}{\hbar} R_B N_n \Delta d,$$

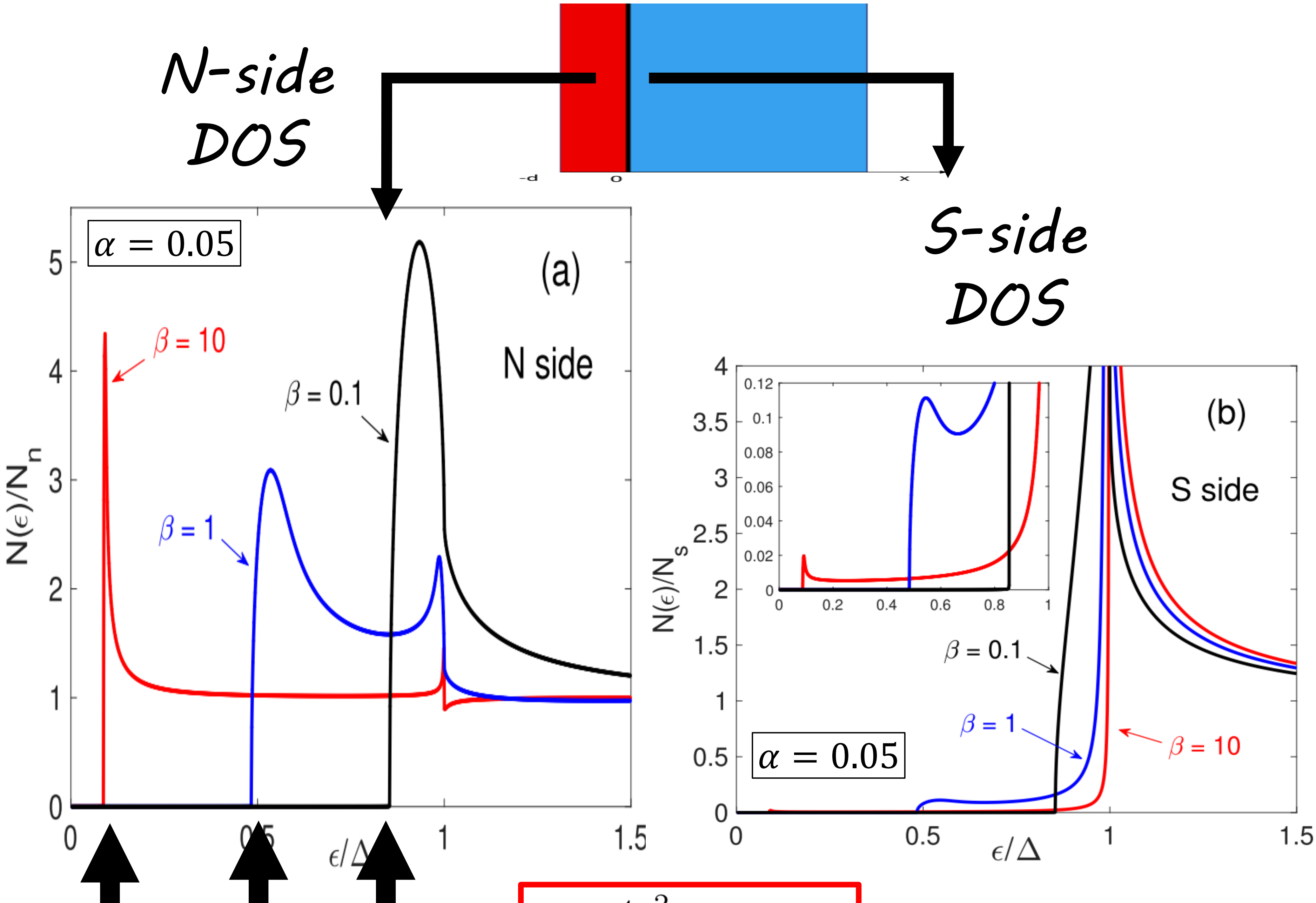

minigap

$$\beta = \frac{4e^2}{\hbar} R_B N_n \Delta d,$$

Taking into account a finite quasi particle life time ($\varepsilon \to \varepsilon + i\Gamma$) smears out the cusps.

N-side DOS

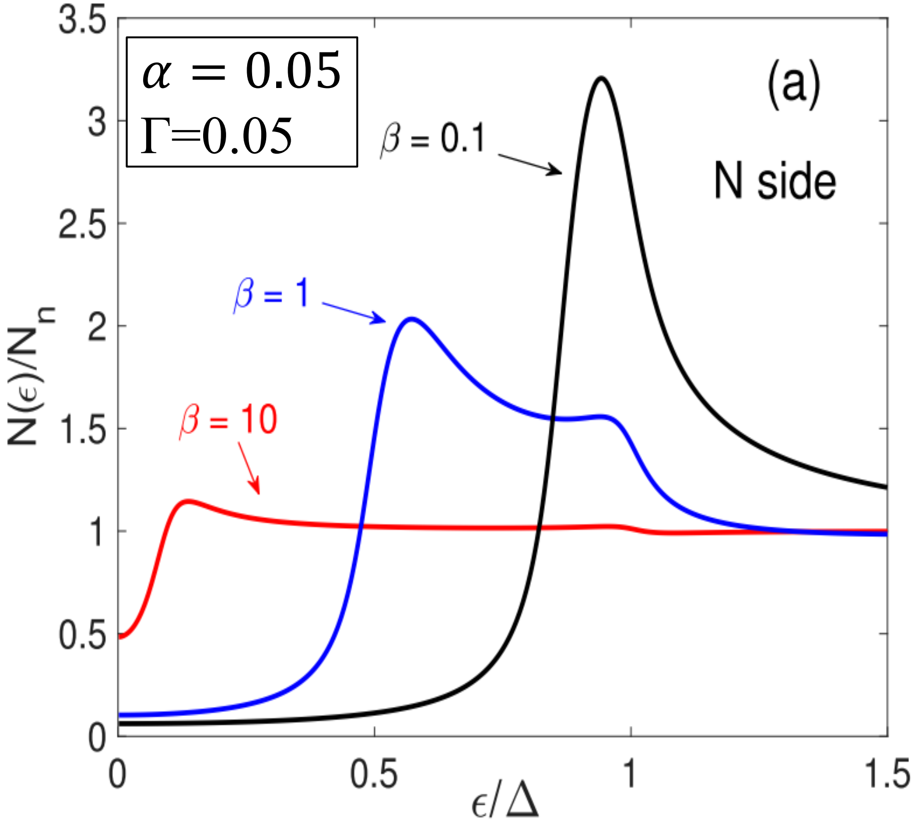

S-side DOS

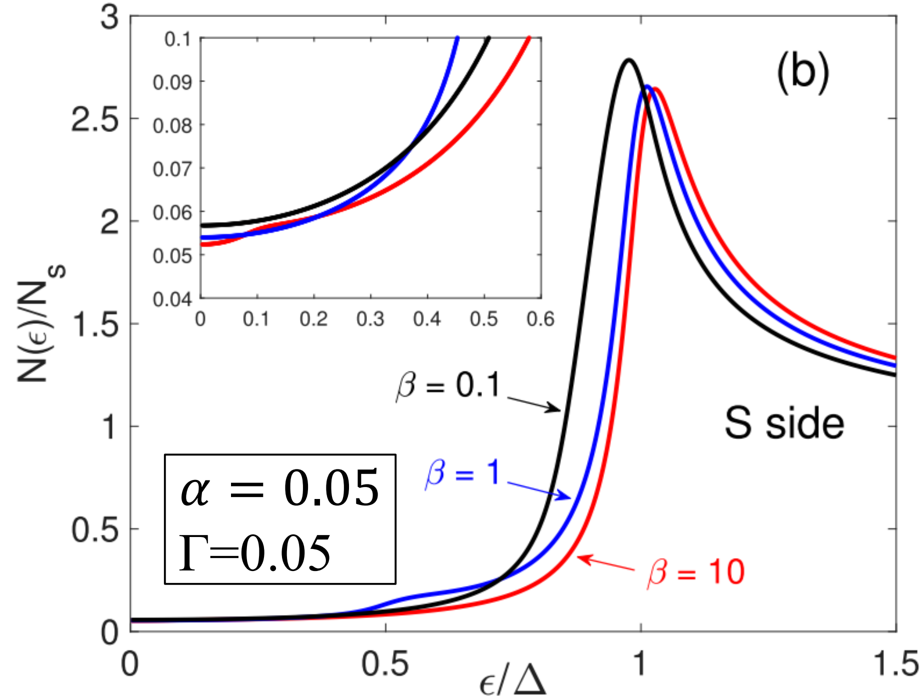

DOS for the right figure (SC with a surface layer of gradually reduced BCS pairing constant) can also be calculated.

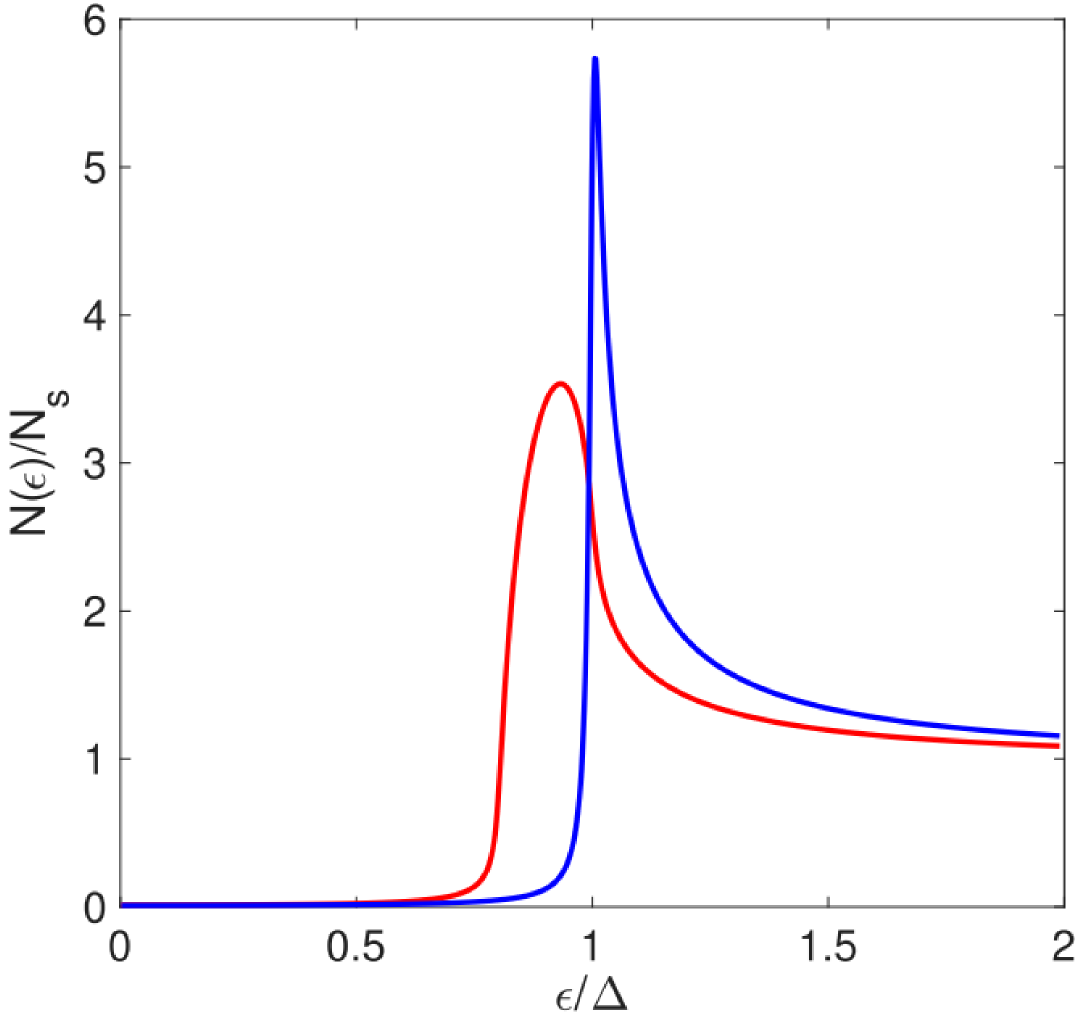

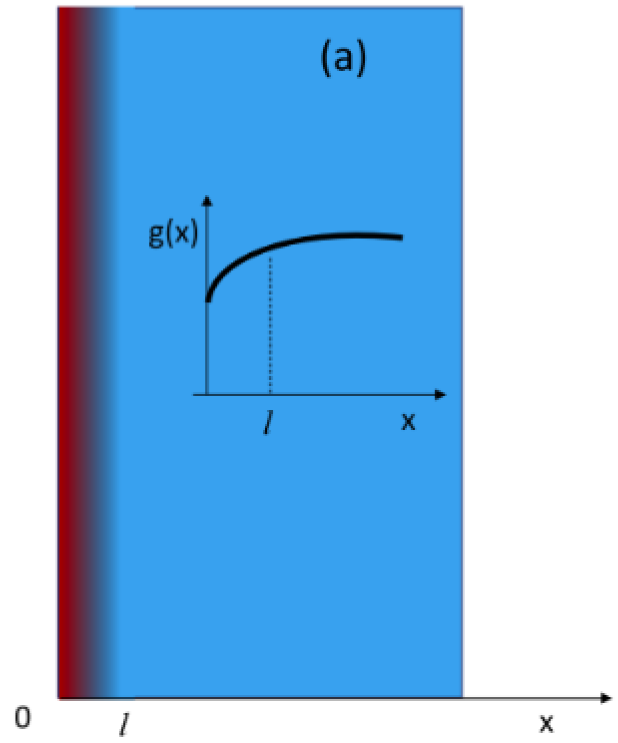

FIG. 2. Density of states at the surface calculated for $\Psi = 0.2$ and $\Gamma = 0.01$ (red line). The blue line shows DOS in the bulk.

Temperature dependence of penetration Depth

Without subgap states

$$\frac{1}{\lambda^2} = \frac{\pi\mu_0\Delta}{\hbar\rho_s}\tanh\frac{\Delta}{2k_BT}$$

Exponential T dependence at any temperature

Without subgap states

$$\frac{1}{\lambda^2} = \frac{\pi\mu_0\Delta}{\hbar\rho_s}\tanh\frac{\Delta}{2k_BT}$$

Exponential T dependence at any temperature

Effect of subgap states

$$\frac{1}{\lambda^2} = \frac{2\mu_0\Delta}{\hbar\rho_s}\left[\tan^{-1}\frac{\Delta}{\Gamma} - \frac{\pi^2k_B^2T^2\Gamma\Delta}{3(\Gamma^2+\Delta^2)^2}\right] \qquad T \ll T_c$$

quadratic T dependence at a low temperature

Surface Resistance

(1)Ideal surface <u>without</u> subgap states
(2)Ideal surface <u>with</u> subgap states
(3)normal thin layer on the surface

Surface Resistance

(1) Ideal surface <u>without</u> subgap states

(2) Ideal surface <u>with</u> subgap states

(3) normal thin layer on the surface

DOS

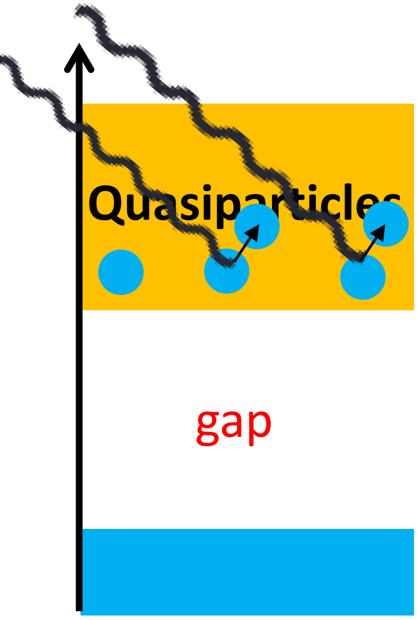
Quasiparticles
gap

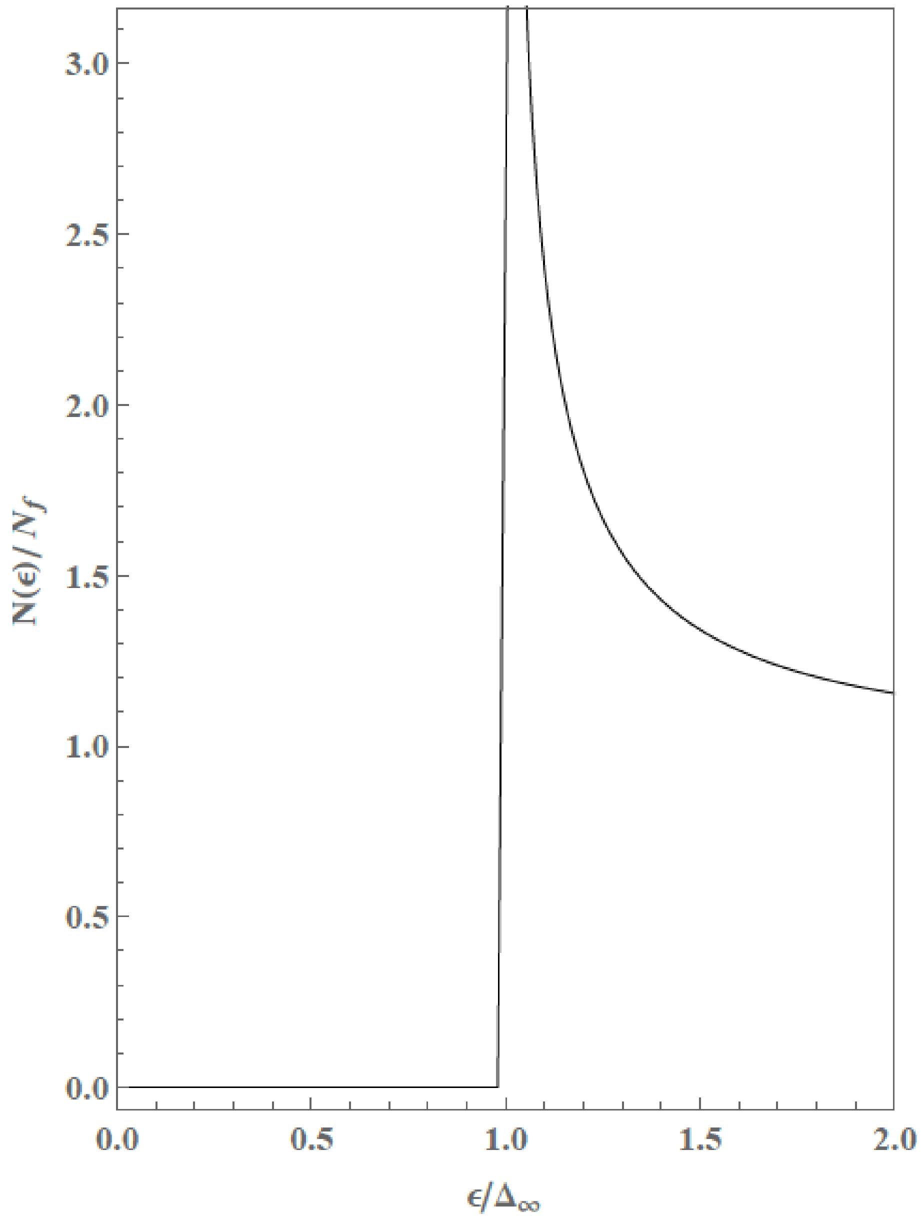
$N(\epsilon)/N_f$
ϵ/Δ_∞
0.0
0.5
1.0
1.5
2.0
2.5
3.0

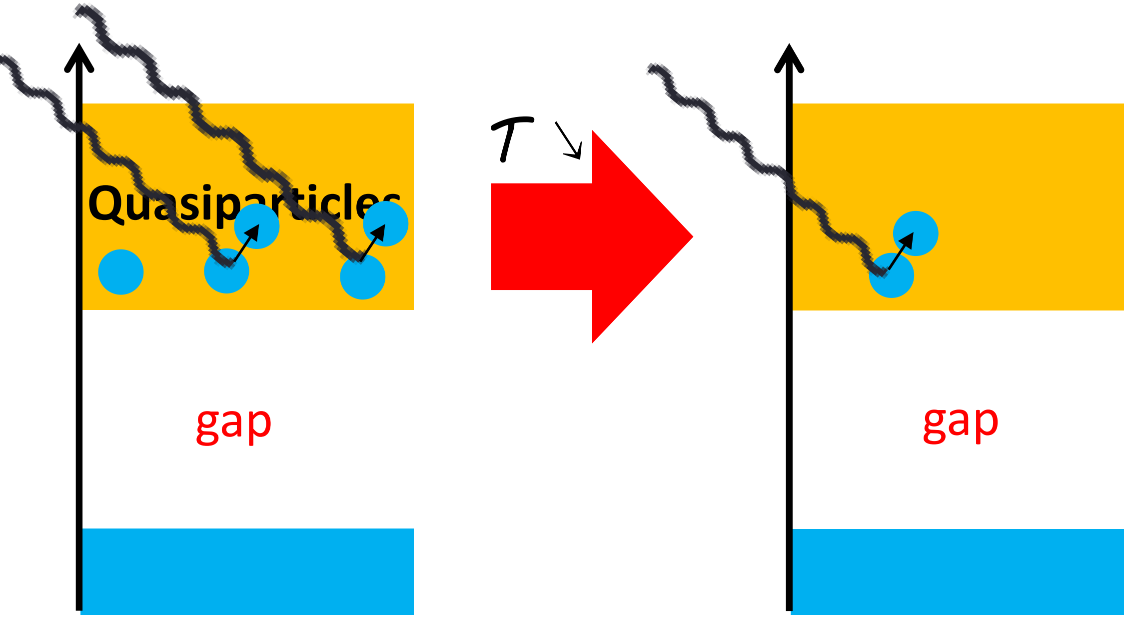

As T decreases, a number of quasiparticles exponentially decrease.

$$R_s \propto e^{-\frac{\Delta}{kT}}$$

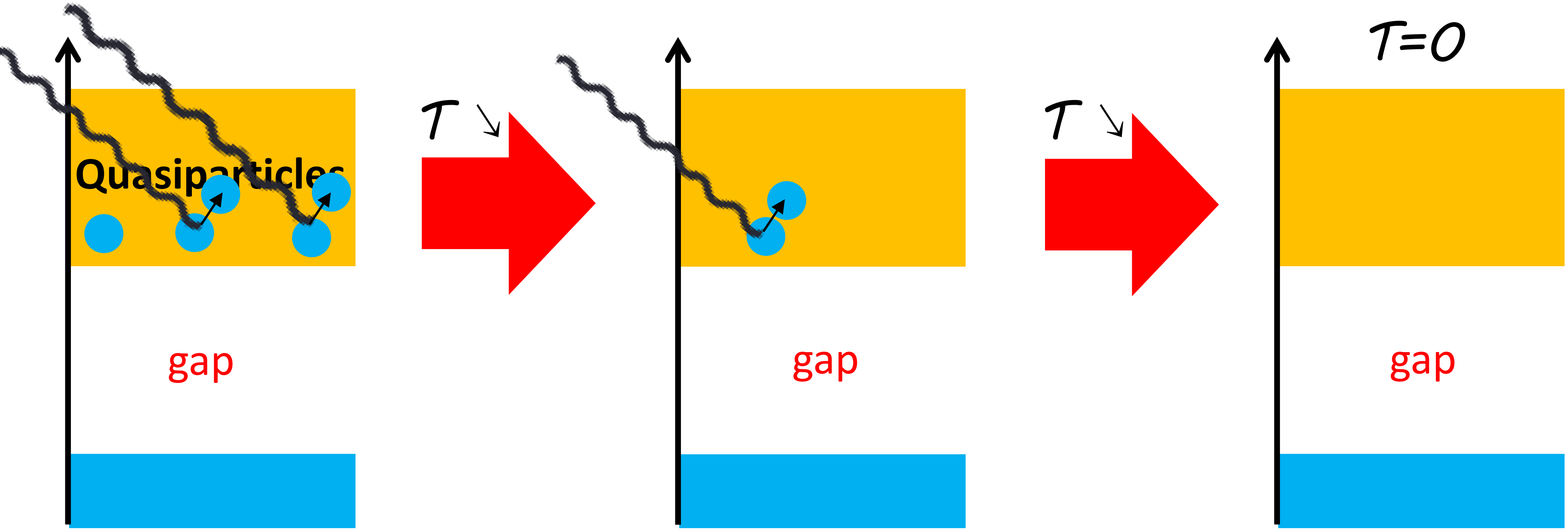

As T decreases, a number of quasiparticles exponentially decrease.

$$R_s \propto e^{-\frac{\Delta}{kT}} \xrightarrow[T\to 0]{} 0 \qquad (R_i = 0)$$

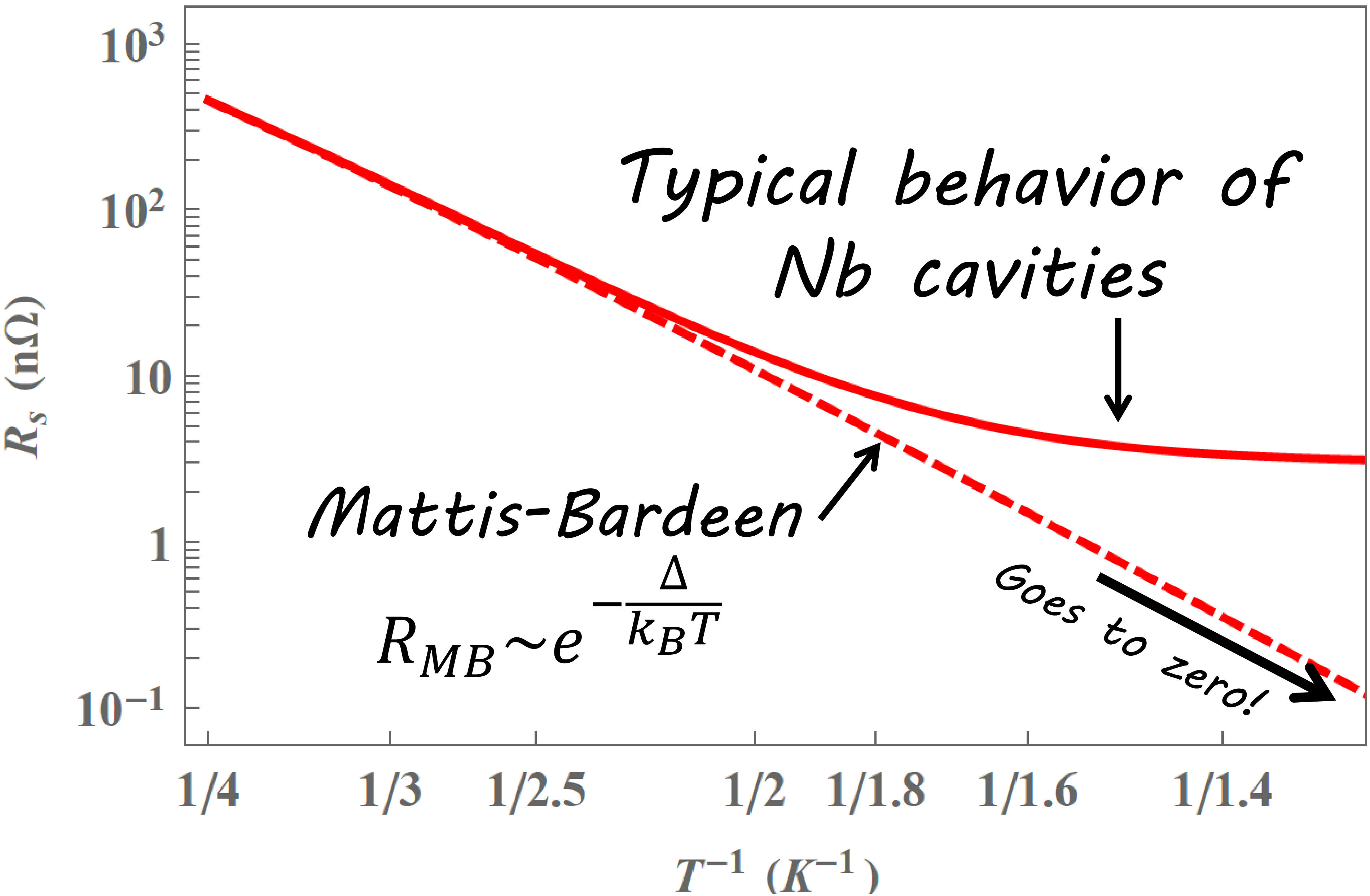

10^3
10^2
10
1
10^{-1}
R_s (nΩ)
Typical behavior of Nb cavities
Mattis-Bardeen
$R_{MB} \sim e^{-\frac{\Delta}{k_B T}}$
Goes to zero!
1/4
1/3
1/2.5
1/2
1/1.8
1/1.6
1/1.4
T^{-1} (K^{-1})

Surface Resistance

(1)Ideal surface without subgap states

(2)Ideal surface with subgap states

(3)normal thin layer on the surface

DOS

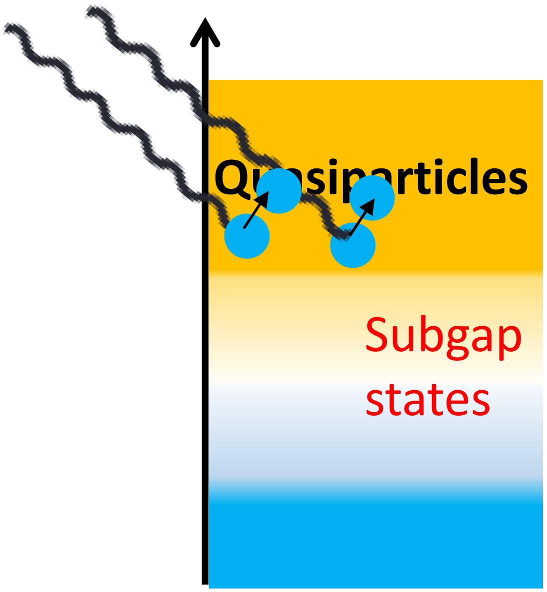
Quasiparticles
Subgap
states

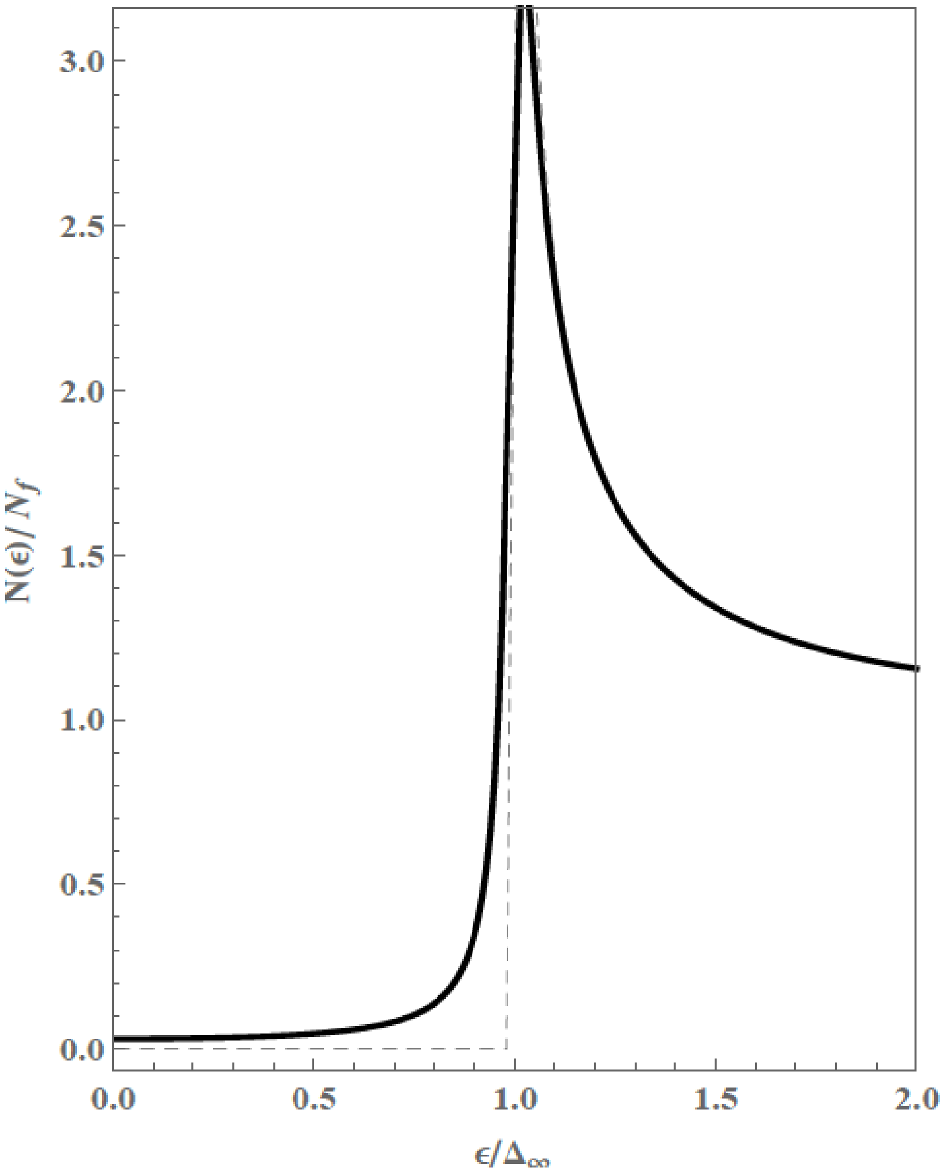
3.0
2.5
2.0
1.5
1.0
0.5
0.0
N(ϵ)/N_f
0.0
0.5
1.0
1.5
2.0
ϵ/Δ_∞

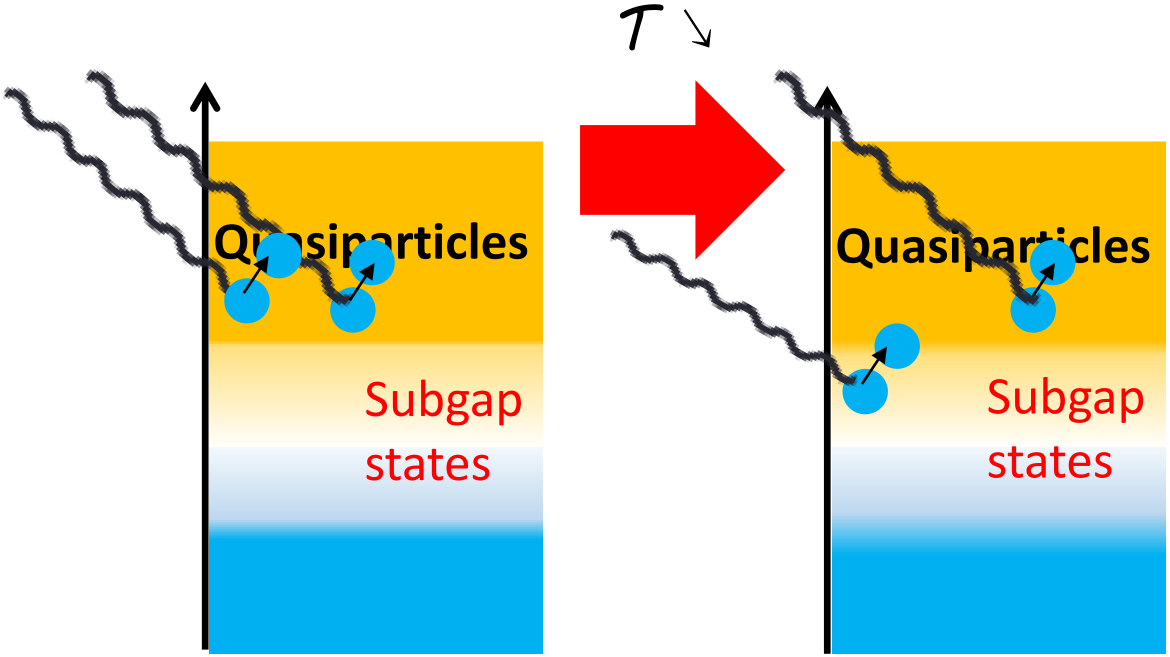
T ↘
Quasiparticles
Subgap states
Quasiparticles
Subgap states

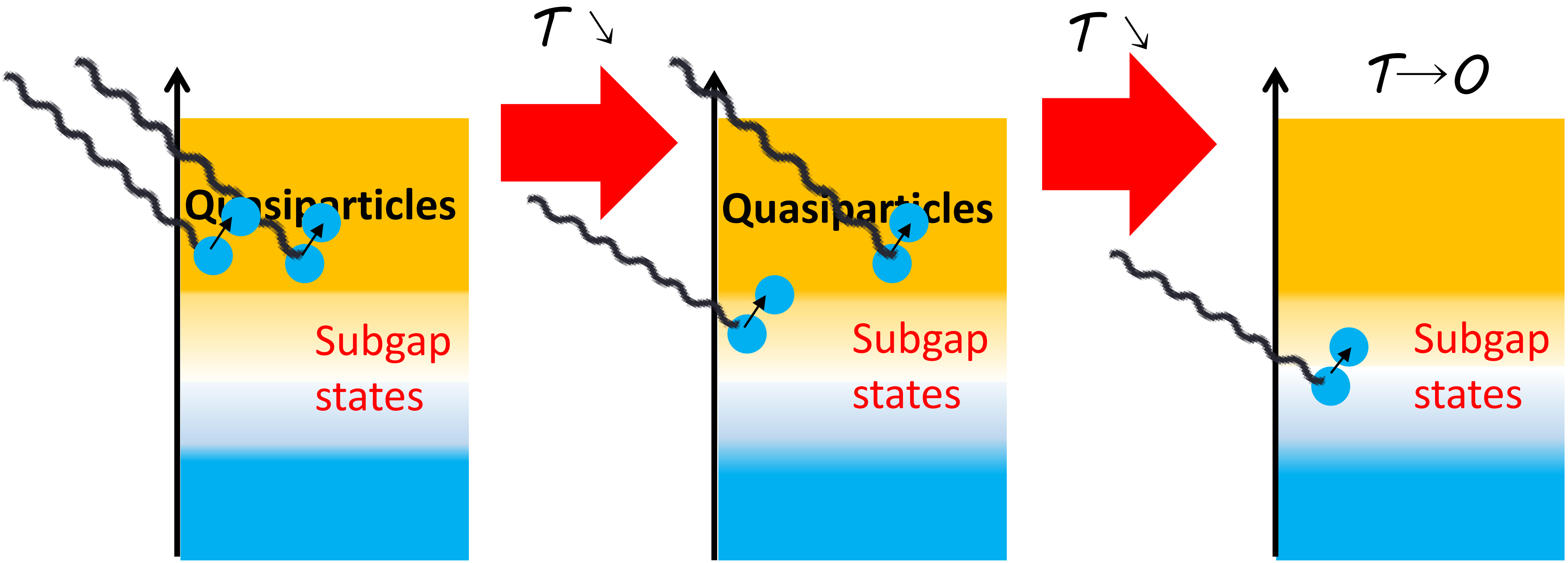

Even at T→0, quasiparticles can be excited by the microwave field when finite subgap states exist.

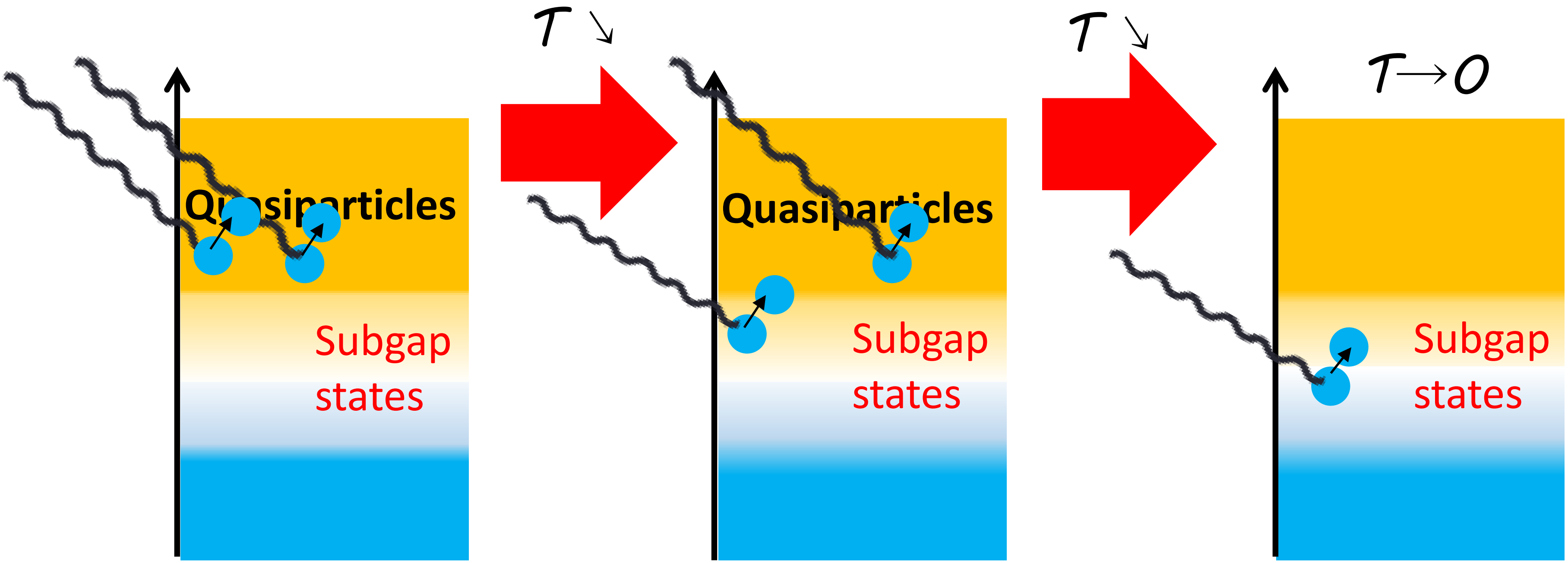

Even at T→0, quasiparticles can be excited by the microwave field when finite subgap states exist.

$$R_i(T) = \frac{\mu_0^2 \omega^2 \lambda^3 \Gamma^2}{2\rho_n(\Delta^2 + \Gamma^2)} \left[1 + \frac{4\pi^2 k_B^2 T^2 \Delta^2}{3(\Delta^2 + \Gamma^2)^2} \right]$$

at $k_B T \lesssim \Gamma$

examples

$$\frac{\Gamma}{\Delta} = 0.06$$

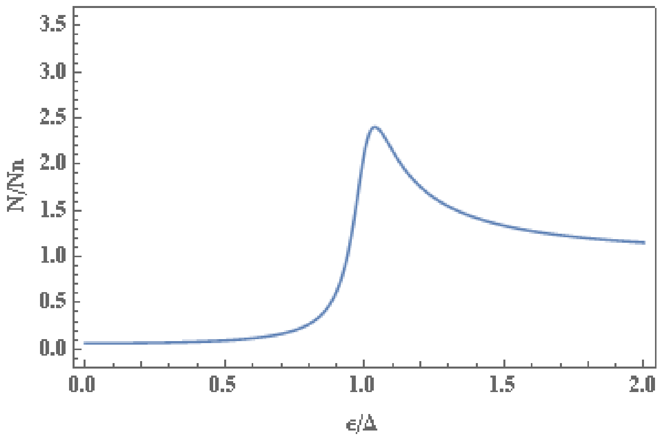

examples

$$\frac{\Gamma}{\Delta} = 0.06$$

$$\frac{\Gamma}{\Delta} = 0.03$$

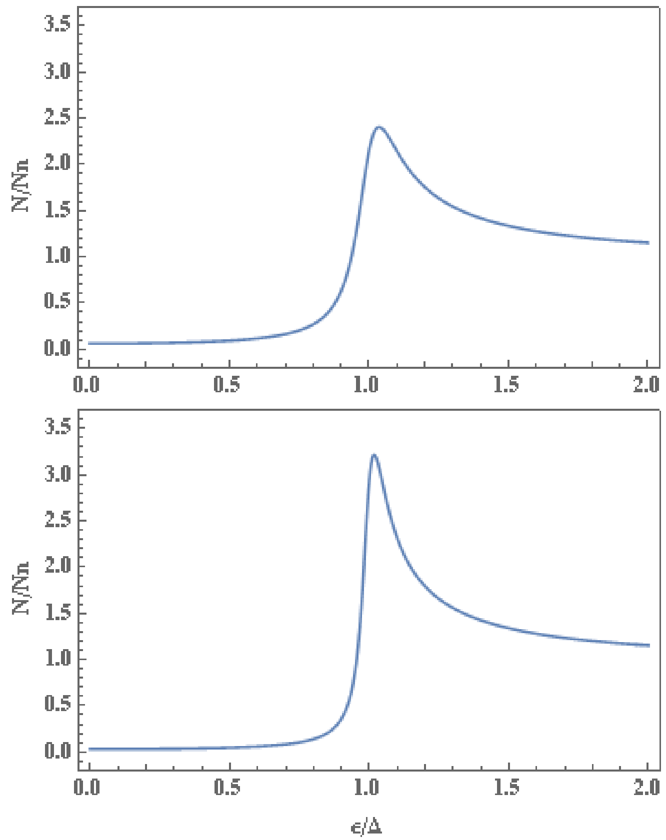

examples

$$\frac{\Gamma}{\Delta} = 0.06$$

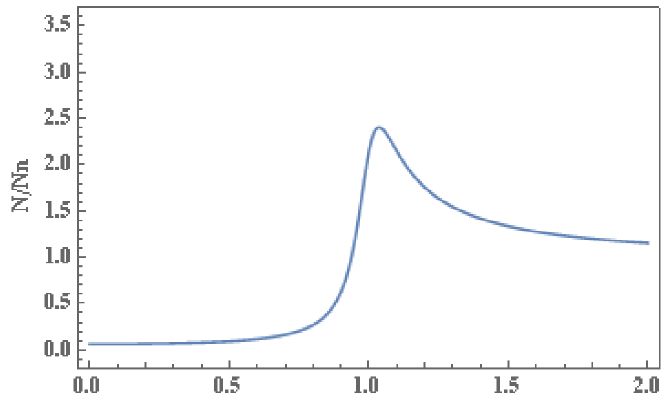

$$\frac{\Gamma}{\Delta} = 0.03$$

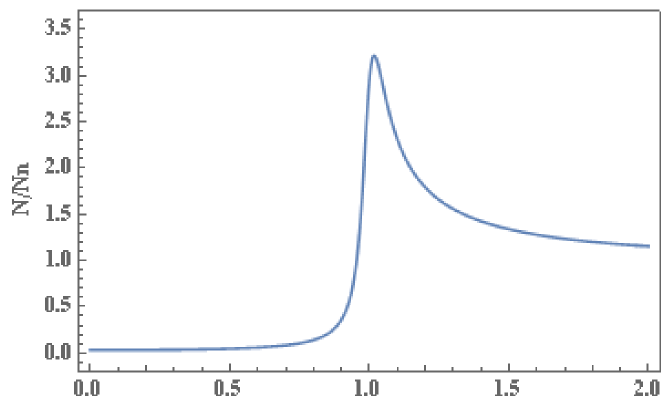

$$\frac{\Gamma}{\Delta} = 0.01$$

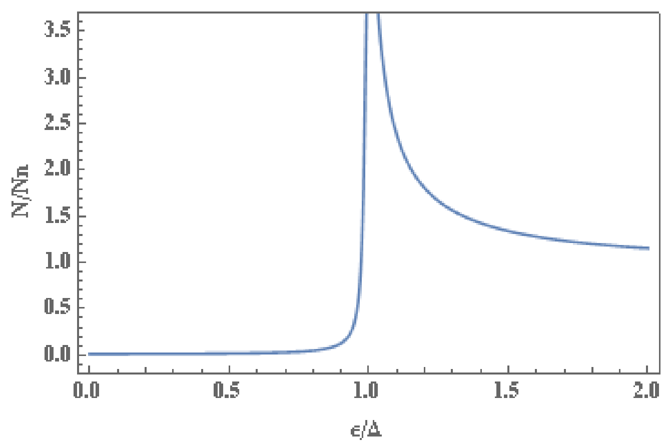

examples

$$\frac{\Gamma}{\Delta} = 0.06$$

$$\frac{\Gamma}{\Delta} = 0.03$$

$$\frac{\Gamma}{\Delta} = 0.01$$

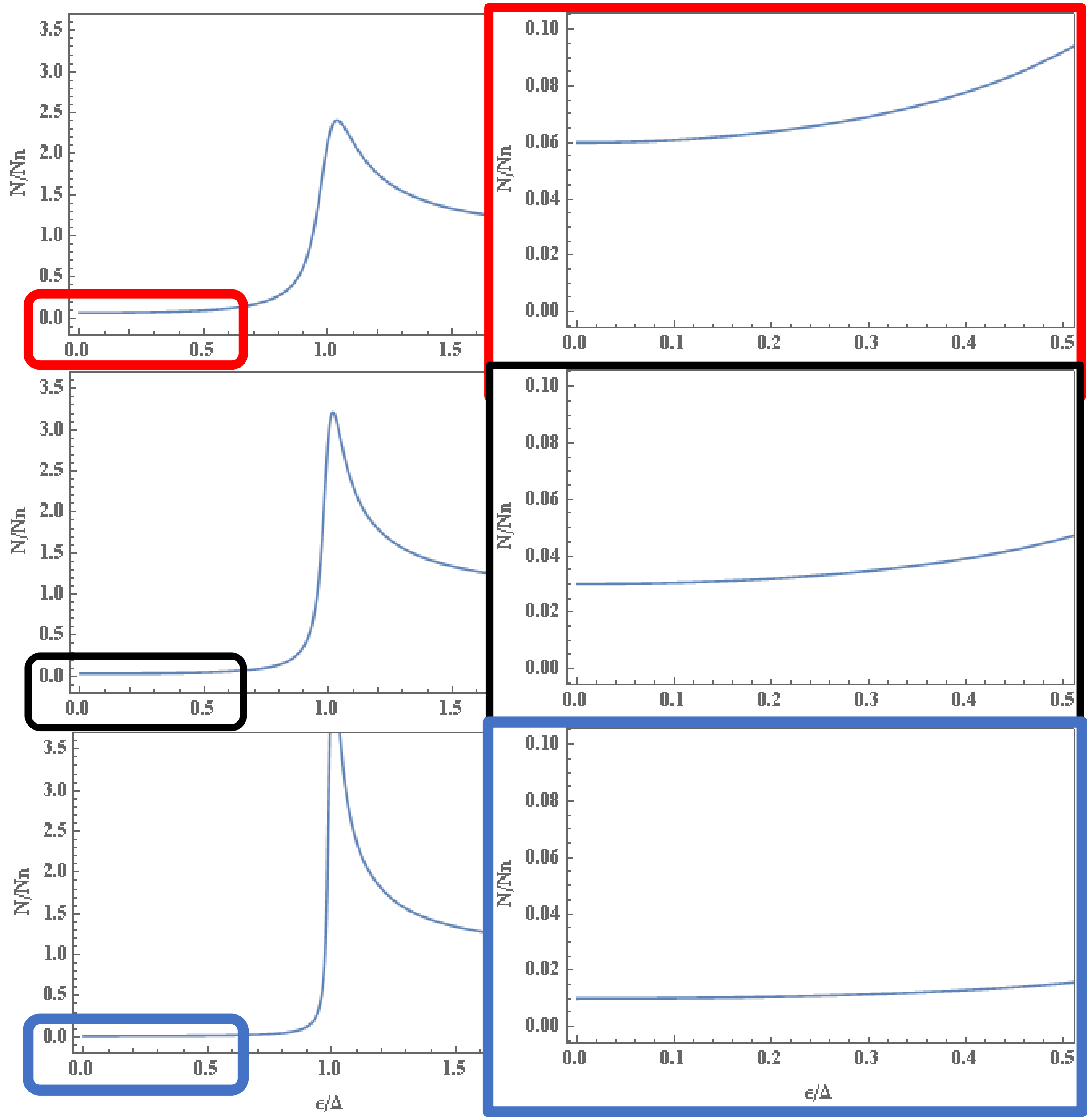

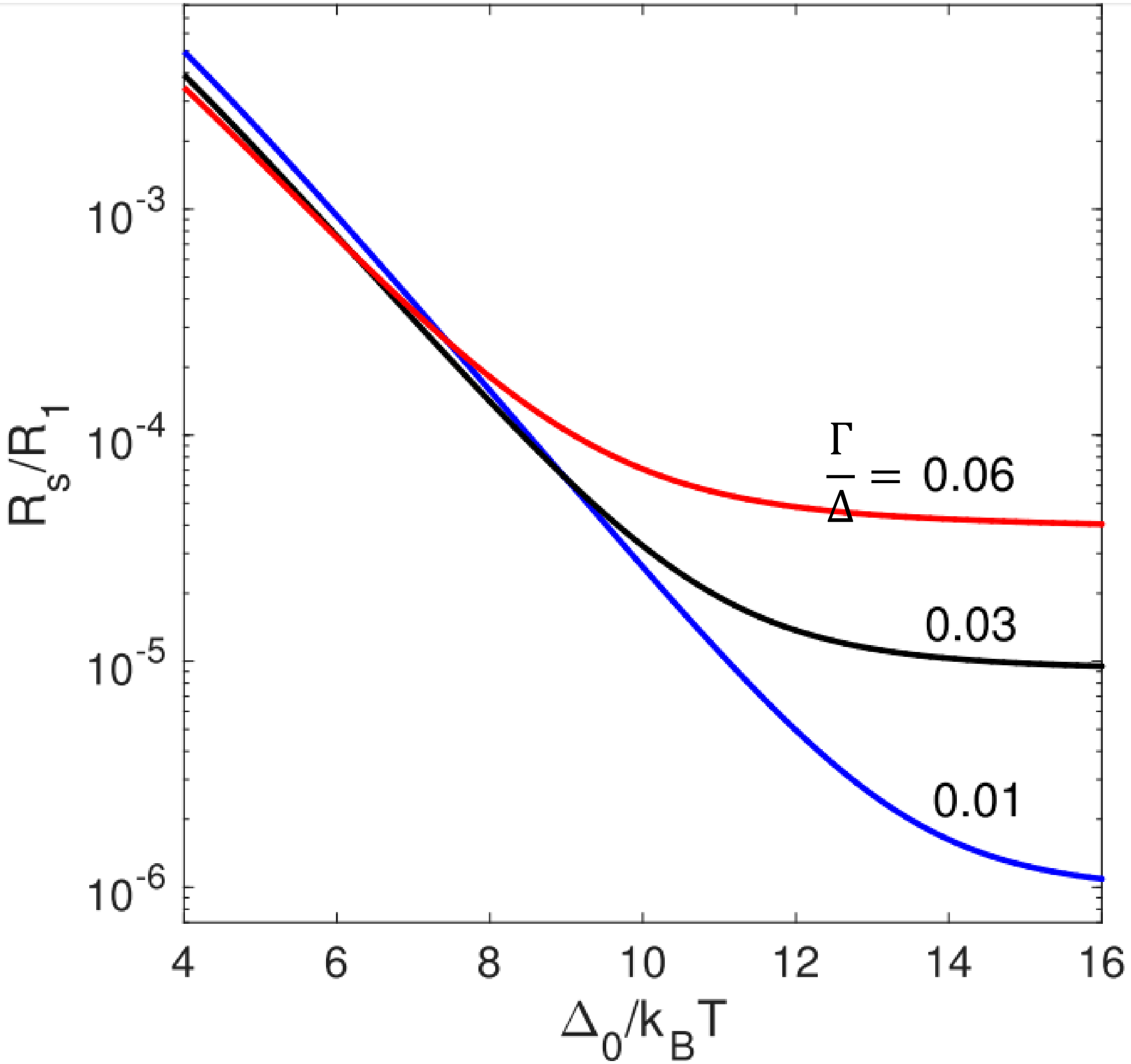

FIG. 7. Arrhenius plots for $R_s(T)$ calculated from Eq. (82)-(83) for $\hbar\omega = 0.01\Delta$ and $\Gamma/\Delta_0 = 0.01$, 0.03 and 0.06. Here $R_1 = \mu_0^2\lambda^3\omega\Delta/2\hbar\rho_s$, the temperature dependencies of Δ and λ at $T < T_c/2$ are neglected, and $\Delta(\Gamma)$ is given by Eq. (20)

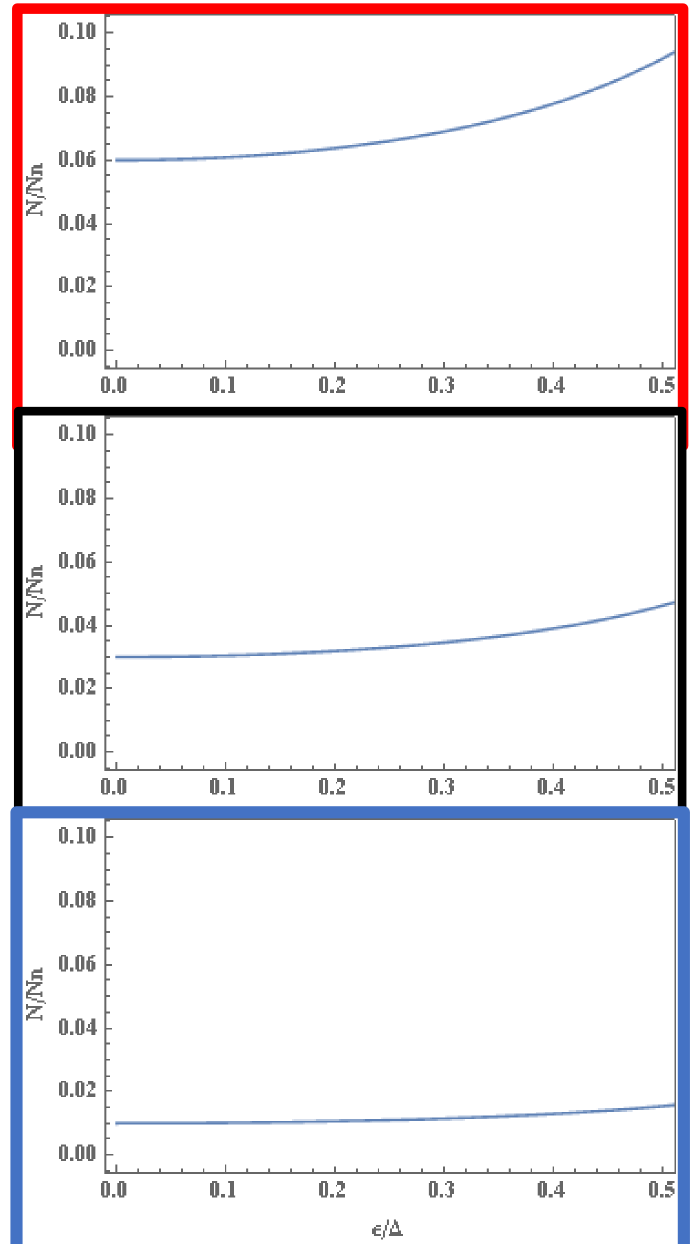

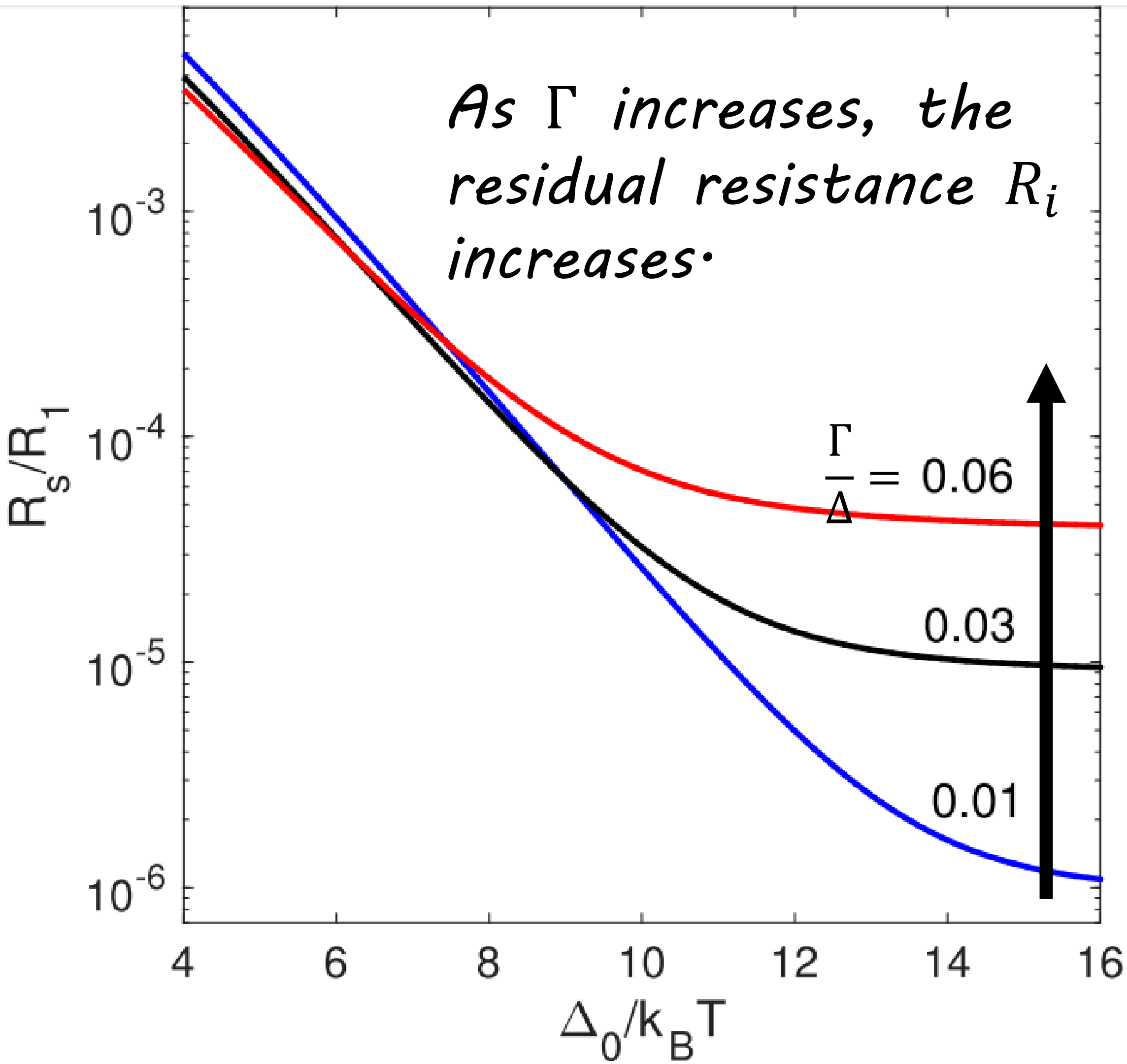

FIG. 7. Arrhenius plots for $R_s(T)$ calculated from Eq. (82)-(83) for $\hbar\omega = 0.01\Delta$ and $\Gamma/\Delta_0 = 0.01, 0.03$ and 0.06. Here $R_1 = \mu_0^2\lambda^3\omega\Delta/2\hbar\rho_s$, the temperature dependencies of Δ and λ at $T < T_c/2$ are neglected, and $\Delta(\Gamma)$ is given by Eq. (20)

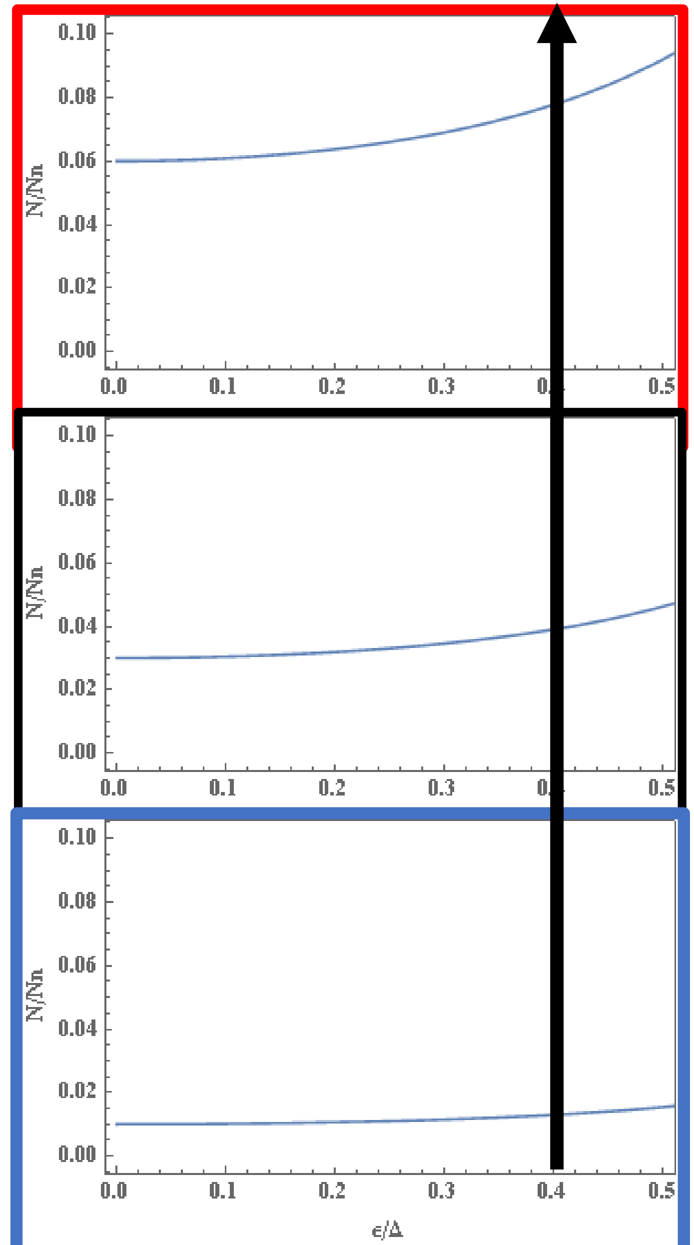

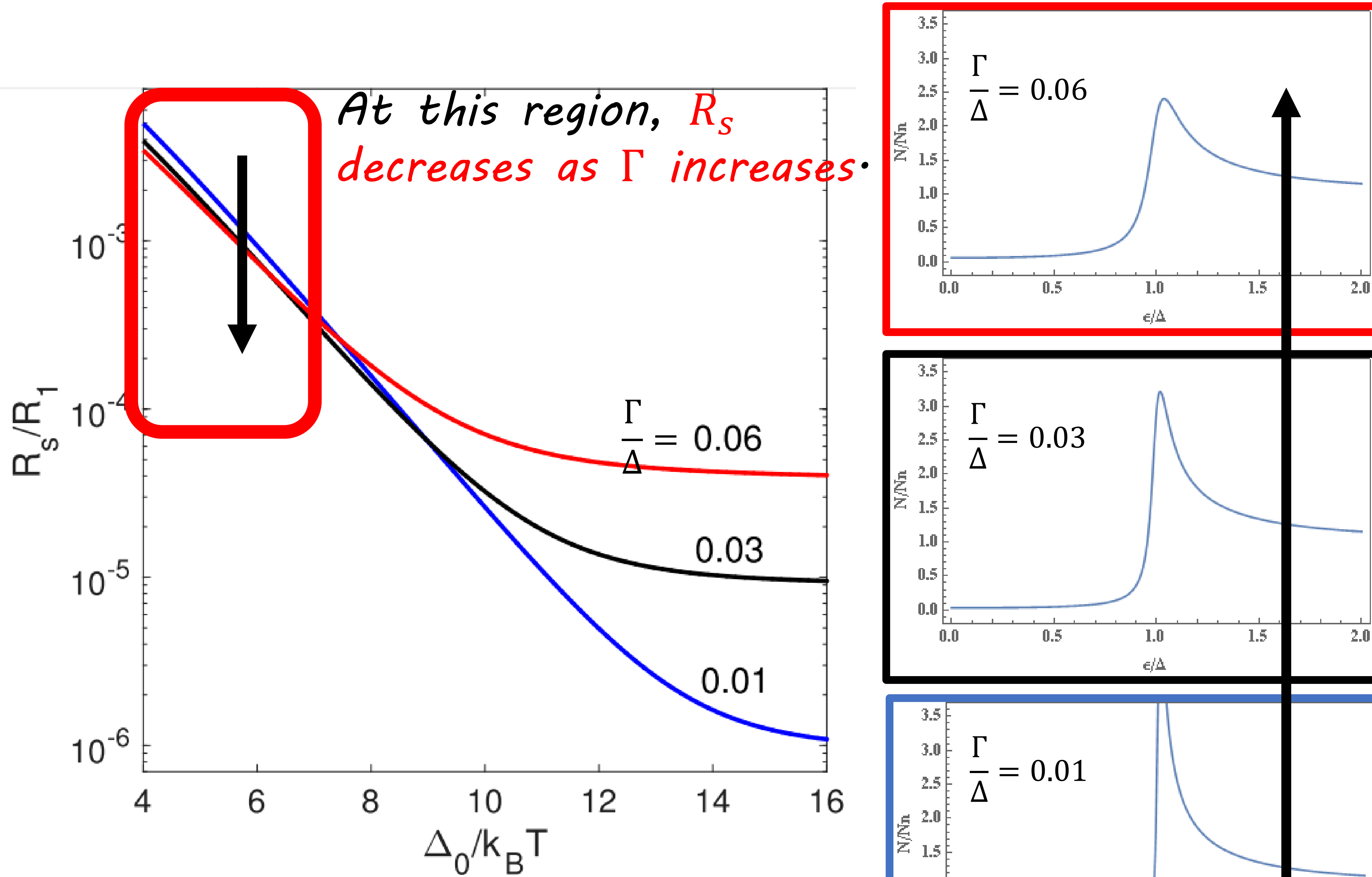

FIG. 7. Arrhenius plots for $R_s(T)$ calculated from Eq. (82)-(83) for $\hbar\omega = 0.01\Delta$ and $\Gamma/\Delta_0 = 0.01$, 0.03 and 0.06. Here $R_1 = \mu_0^2\lambda^3\omega\Delta/2\hbar\rho_s$, the temperature dependencies of Δ and λ at $T < T_c/2$ are neglected, and $\Delta(\Gamma)$ is given by Eq. (20)

Why does R_s decrease as Γ increases?

A. Gurevich, Phys. Rev. Lett. **113**, 087001 (2014)
A. Gurevich, Supercond. Sci. Technol. **30**, 034004 (2017)

Since

$$R_s \sim \int d\epsilon\, N(\epsilon) N(\epsilon + \hbar\omega) e^{-\epsilon/kT}$$

we have

$$R_s \propto \ln \frac{kT}{\hbar\omega}$$

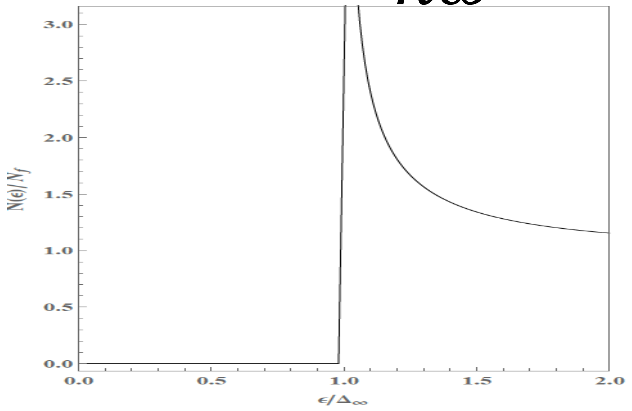

Why does R_s decrease as Γ increases?

A. Gurevich, Phys. Rev. Lett. **113**, 087001 (2014)
A. Gurevich, Supercond. Sci. Technol. **30**, 034004 (2017)

Since

$$R_s \sim \int d\epsilon\, N(\epsilon) N(\epsilon + \hbar\omega) e^{-\epsilon/kT}$$

we have

$$R_s \propto \ln \frac{kT}{\hbar\omega} \quad > \quad R_s \propto \ln \frac{kT}{\Gamma}$$

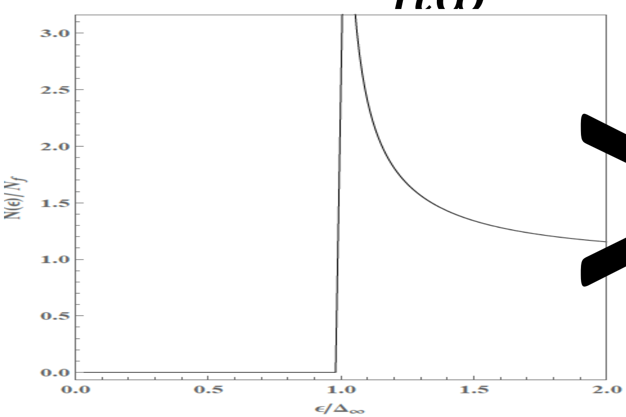

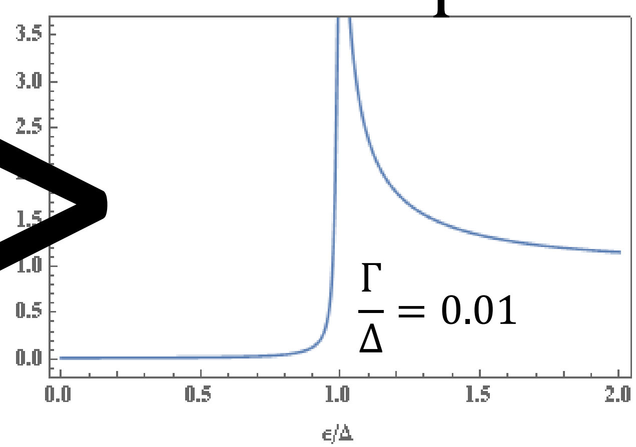

$$\frac{\Gamma}{\Delta} = 0.01$$

Why does R_s decrease as Γ increases?

A. Gurevich, Phys. Rev. Lett. **113**, 087001 (2014)
A. Gurevich, Supercond. Sci. Technol. **30**, 034004 (2017)

Since

$$R_s \sim \int d\epsilon\, N(\epsilon) N(\epsilon + \hbar\omega) e^{-\epsilon/kT}$$

we have

$$R_s \propto \ln \frac{kT}{\hbar\omega} \qquad\qquad R_s \propto \ln \frac{kT}{\Gamma}$$

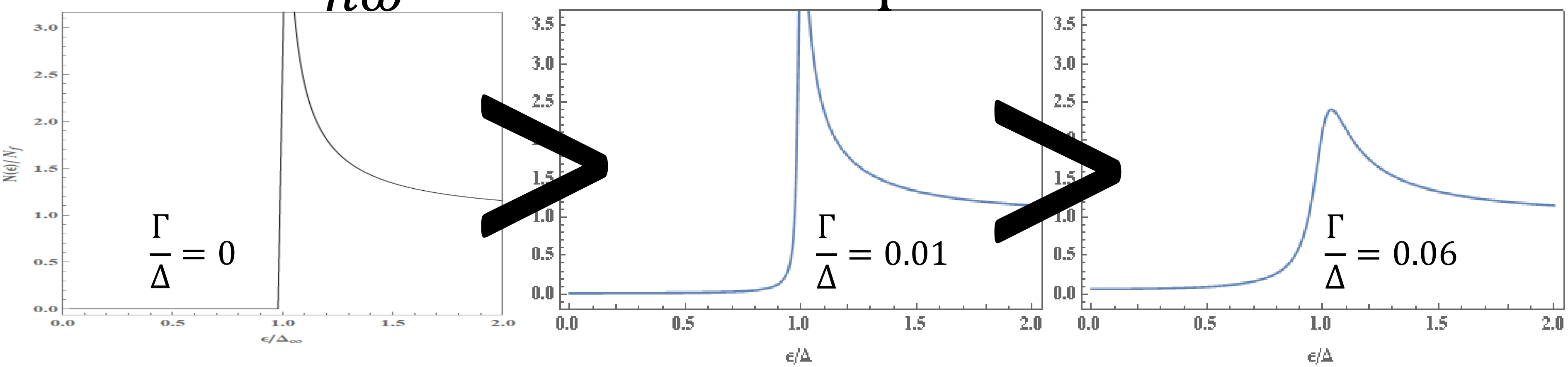

DOS broadening can reduce R_s

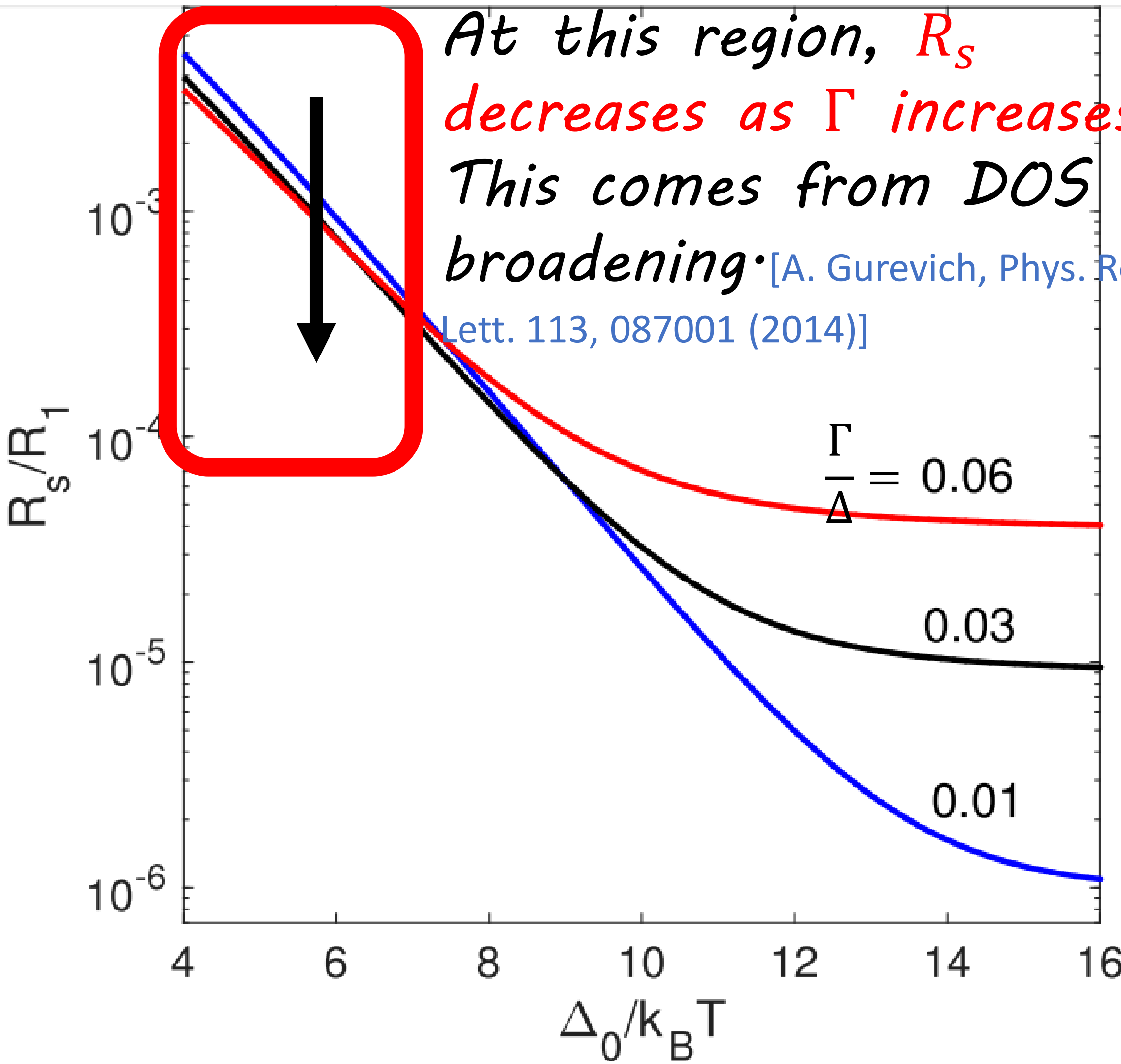

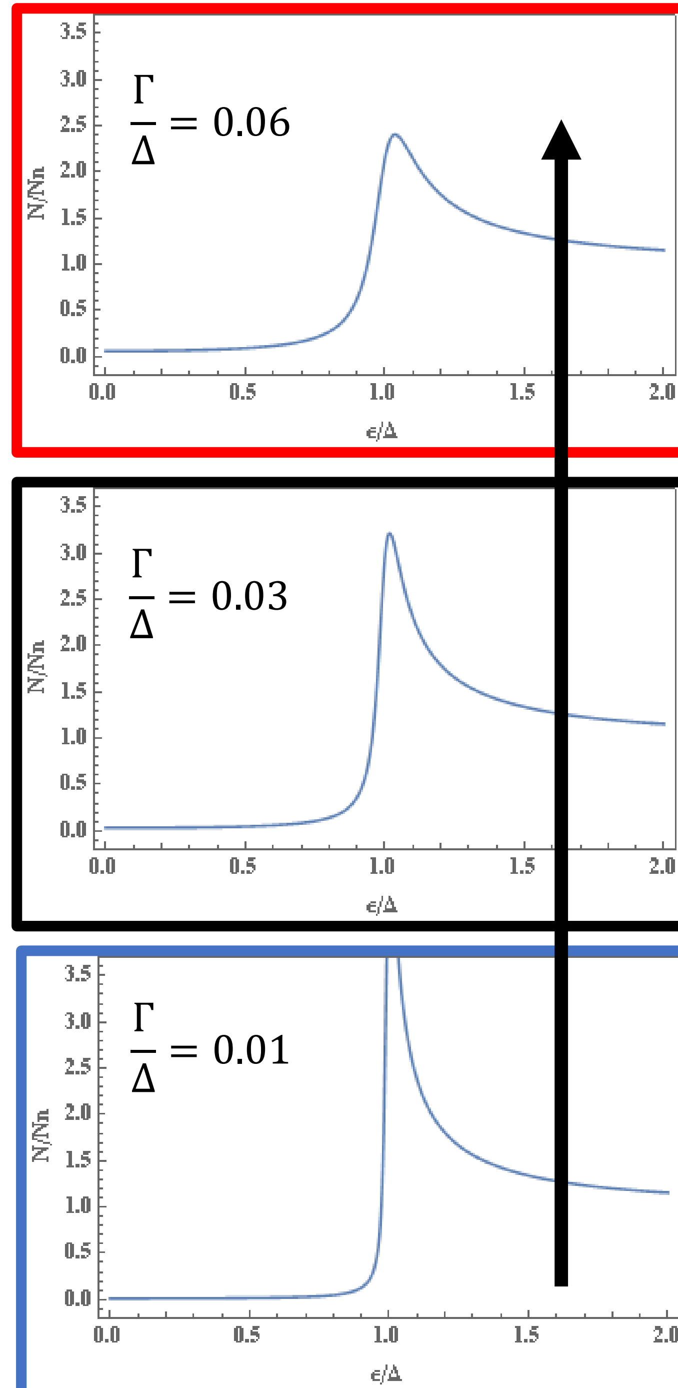

FIG. 7. Arrhenius plots for $R_s(T)$ calculated from Eq. (82)-(83) for $\hbar\omega = 0.01\Delta$ and $\Gamma/\Delta_0 = 0.01$, 0.03 and 0.06. Here $R_1 = \mu_0^2\lambda^3\omega\Delta/2\hbar\rho_s$, the temperature dependencies of Δ and λ at $T < T_c/2$ are neglected, and $\Delta(\Gamma)$ is given by Eq. (20)

Surface Resistance

(1)Ideal surface <u>without</u> subgap states

(2)Ideal surface <u>with</u> subgap states

(3)normal thin layer on the surface

As seen in the above,
DOS is broaden due to proximity effect.
Thus we can expect R_s can be reduced by the same mechanism as before: R_s reduction by the broadening of DOS peak.

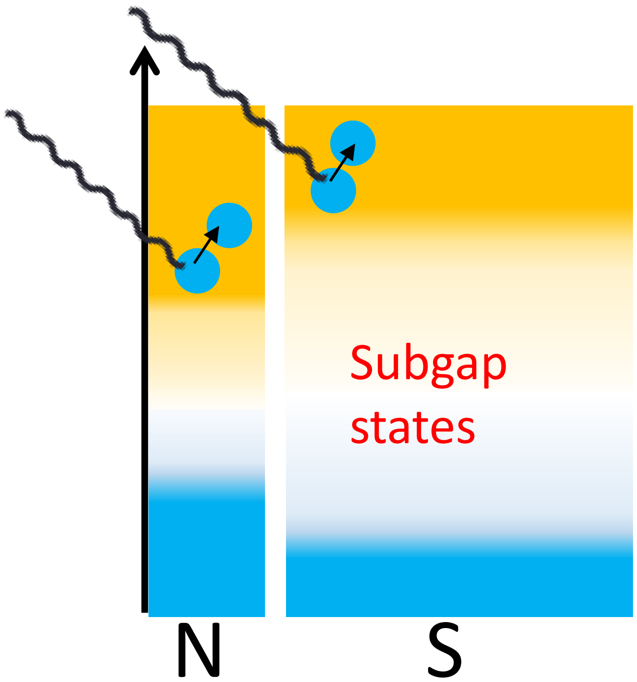
Subgap
states
N
S

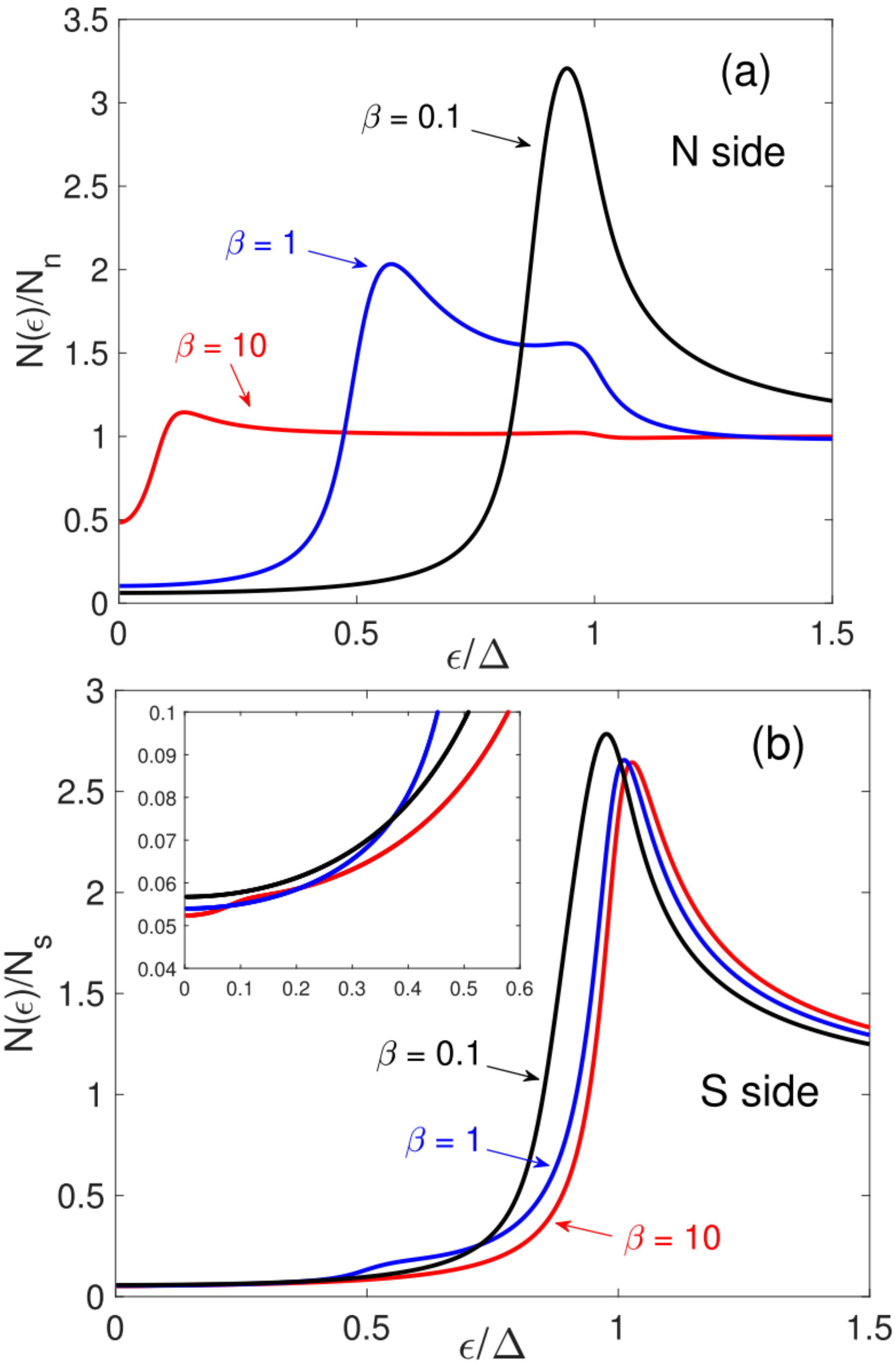
(a)
N side
β = 0.1
β = 1
β = 10
$N(\epsilon)/N_n$
ϵ/Δ
(b)
S side
β = 0.1
β = 1
β = 10
$N(\epsilon)/N_s$
ϵ/Δ

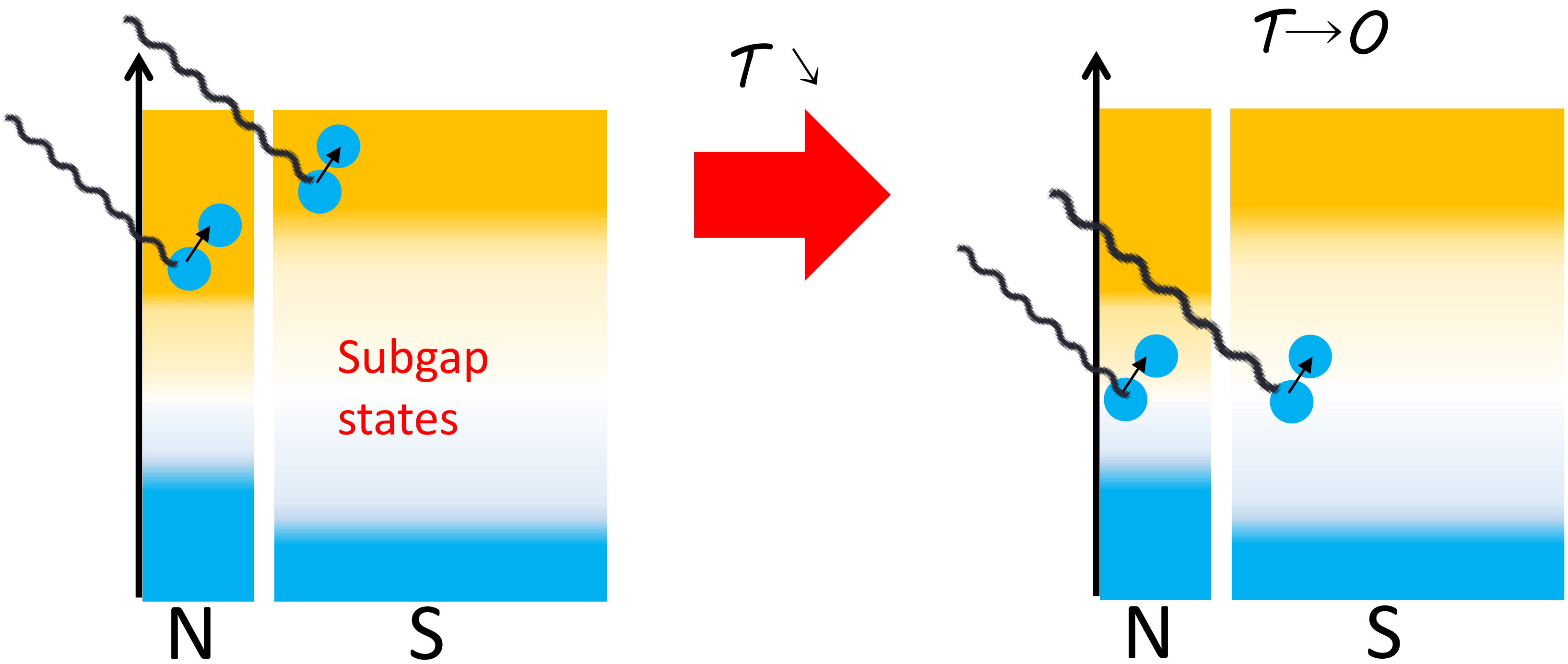

Even at $T \to 0$, quasiparticles can be excited by the microwave field when finite subgap states exist.

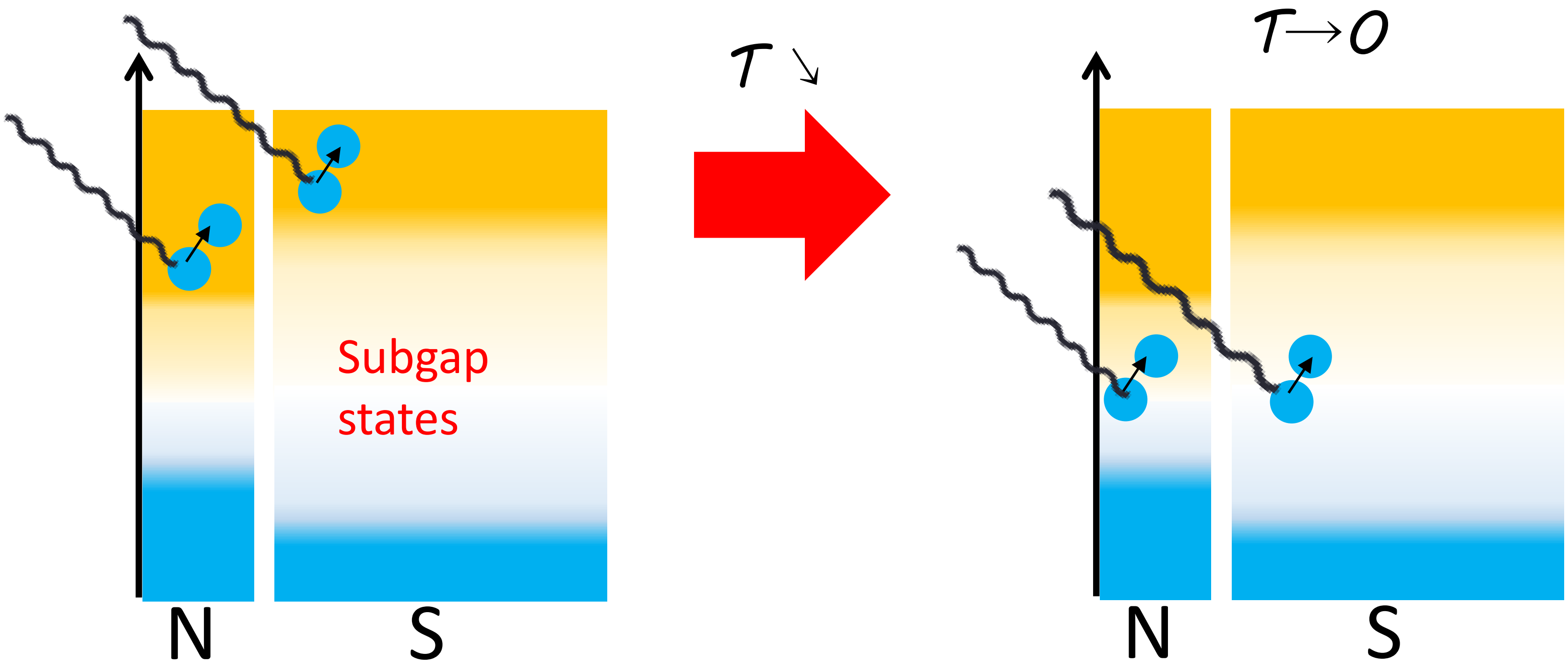

Even at T→0, quasiparticles can be excited by the microwave field when finite subgap states exist.

$$R_i = \frac{1}{2}\mu_0^2\omega^2\lambda^3\sigma_s\left[\frac{\Gamma^2}{\Delta^2+\Gamma^2}+\frac{\tilde{\alpha}\Gamma^2\left(\Delta+\beta\sqrt{\Delta^2+\Gamma^2}\right)^2}{(\Delta^2+\beta^2\Gamma^2)(\Delta^2+\Gamma^2)+2\beta\Gamma^2\Delta\sqrt{\Delta^2+\Gamma^2}}\right]$$

R_s as functions of T^{-1}

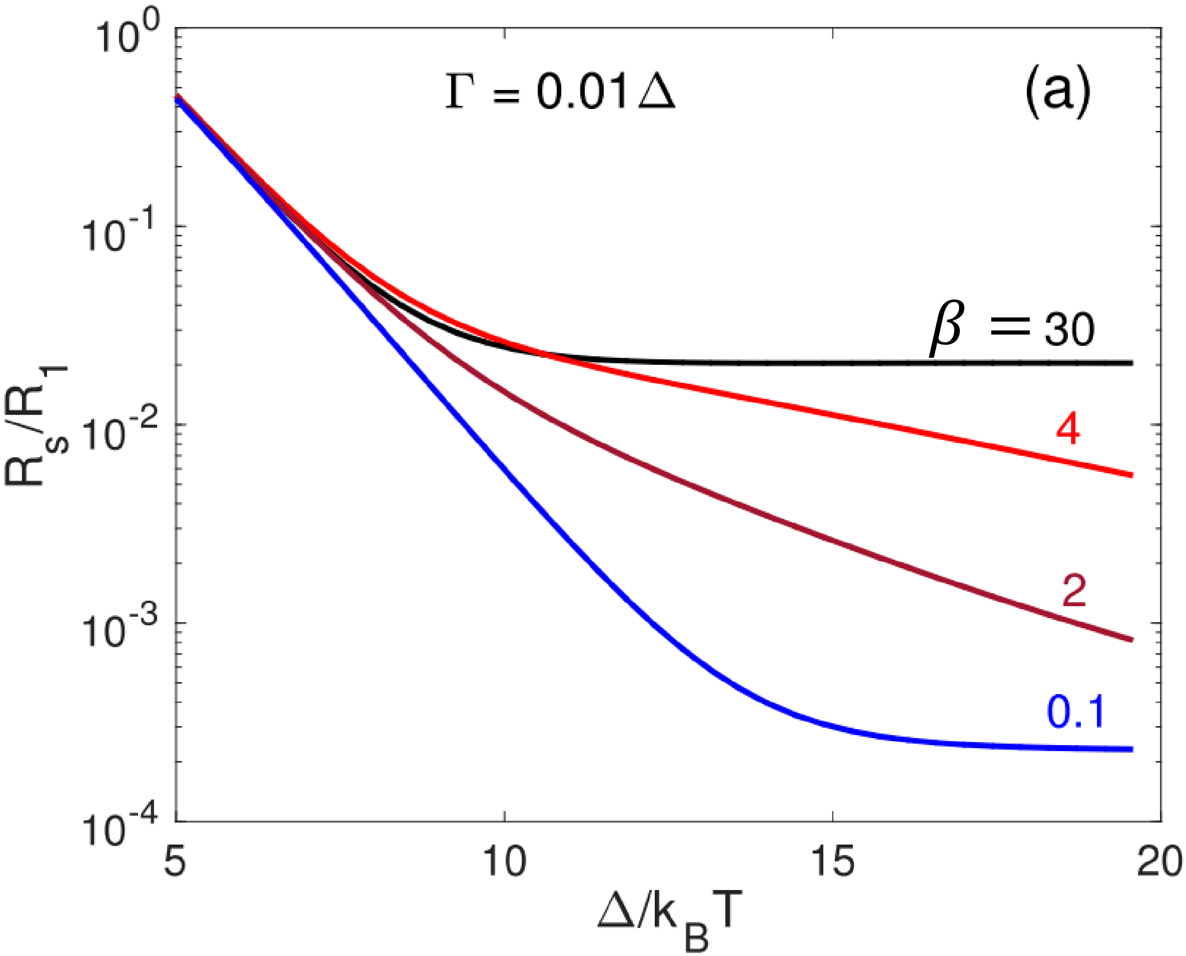

FIG. 10. Arrhenius plots calculated from Eqs. (79)-(81) for $\alpha = 0.05$, $\lambda = 4\xi_S$, $\hbar\Omega = 11\Delta$, $D_n = D_s/3$, $\beta = 0.1,\ 2,\ 4,\ 30$, and (a) $\Gamma = 0.01\Delta$, (b) $\Gamma = 0.05\Delta$. Here $R_1 = \mu_0^2\omega^2\xi_S\lambda^2/2\rho_s$.

R_s as functions of T^{-1}

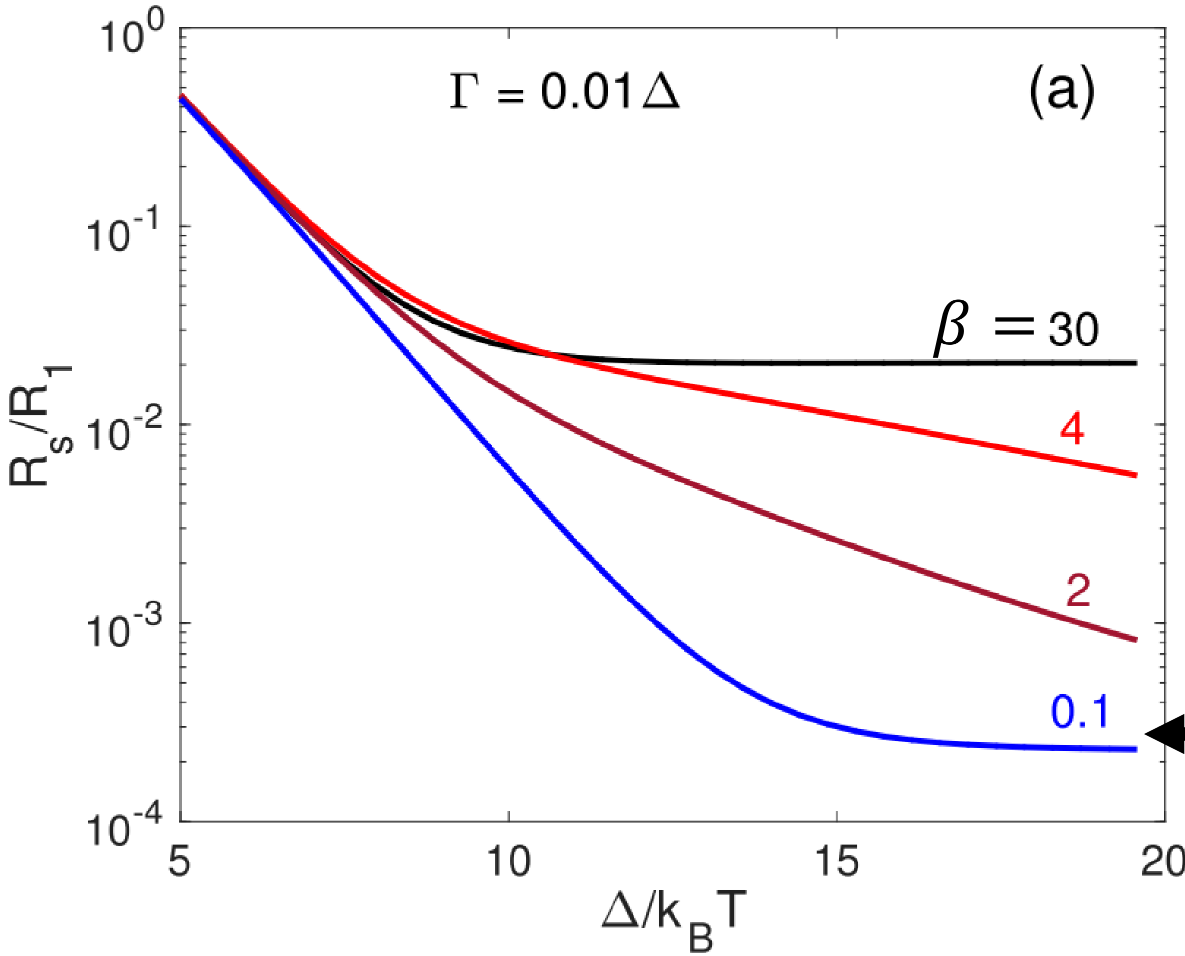

Similar as the ideal surface with subgap states

FIG. 10. Arrhenius plots calculated from Eqs. (79)-(81) for $\alpha = 0.05$, $\lambda = 4\xi_S$, $\hbar\Omega = 11\Delta$, $D_n = D_s/3$, $\beta = 0.1,\ 2,\ 4,\ 30$, and (a) $\Gamma = 0.01\Delta$, (b) $\Gamma = 0.05\Delta$. Here $R_1 = \mu_0^2\omega^2\xi_S\lambda^2/2\rho_s$.

R_s as functions of T^{-1}

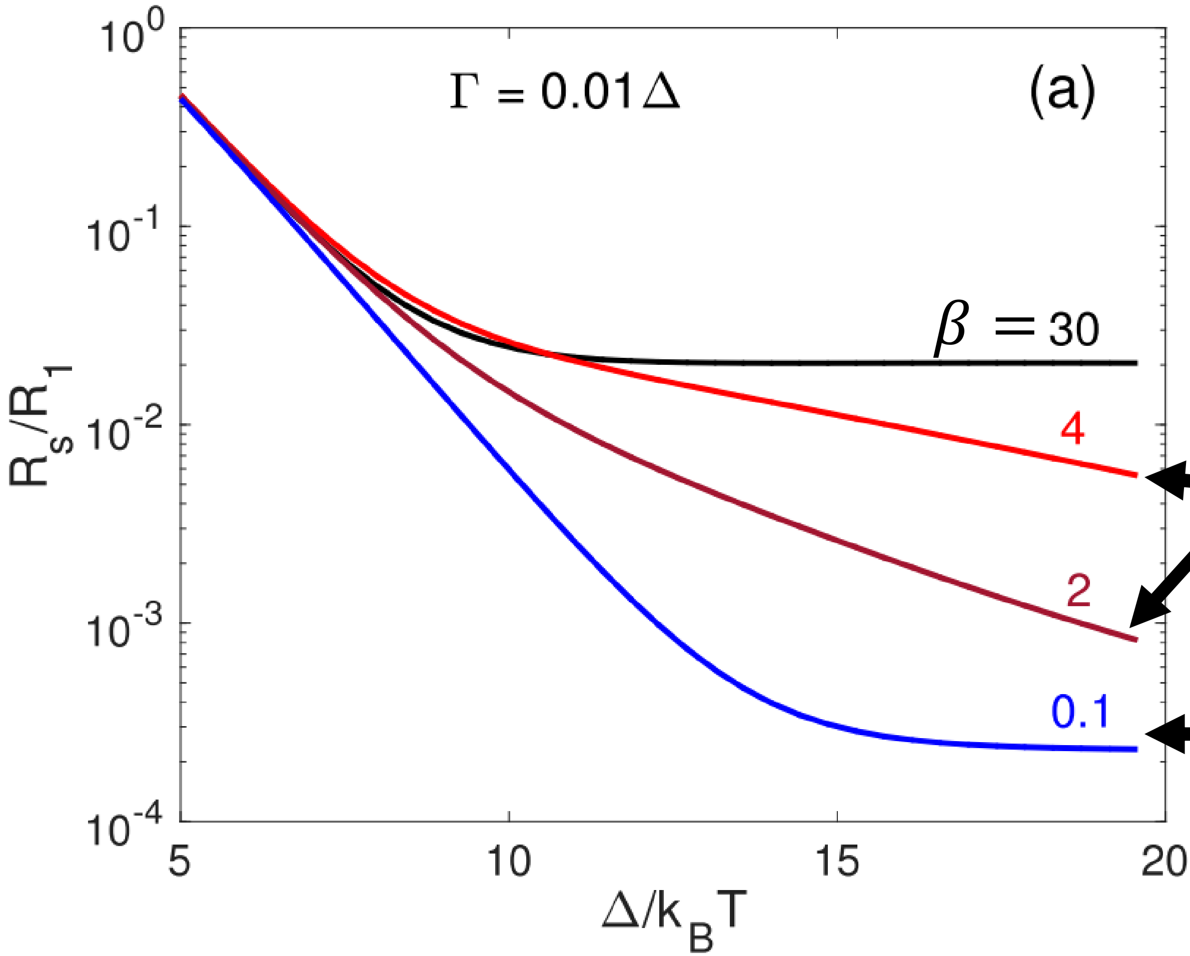

The slope is changed to that corresponding to the minigap

Similar as the ideal surface with subgap states

FIG. 10. Arrhenius plots calculated from Eqs. (79)-(81) for $\alpha = 0.05$, $\lambda = 4\xi_S$, $\hbar\Omega = 11\Delta$, $D_n = D_s/3$, $\beta = 0.1,\ 2,\ 4,\ 30$, and (a) $\Gamma = 0.01\Delta$, (b) $\Gamma = 0.05\Delta$. Here $R_1 = \mu_0^2\omega^2\xi_S\lambda^2/2\rho_s$.

R_s as functions of T^{-1}

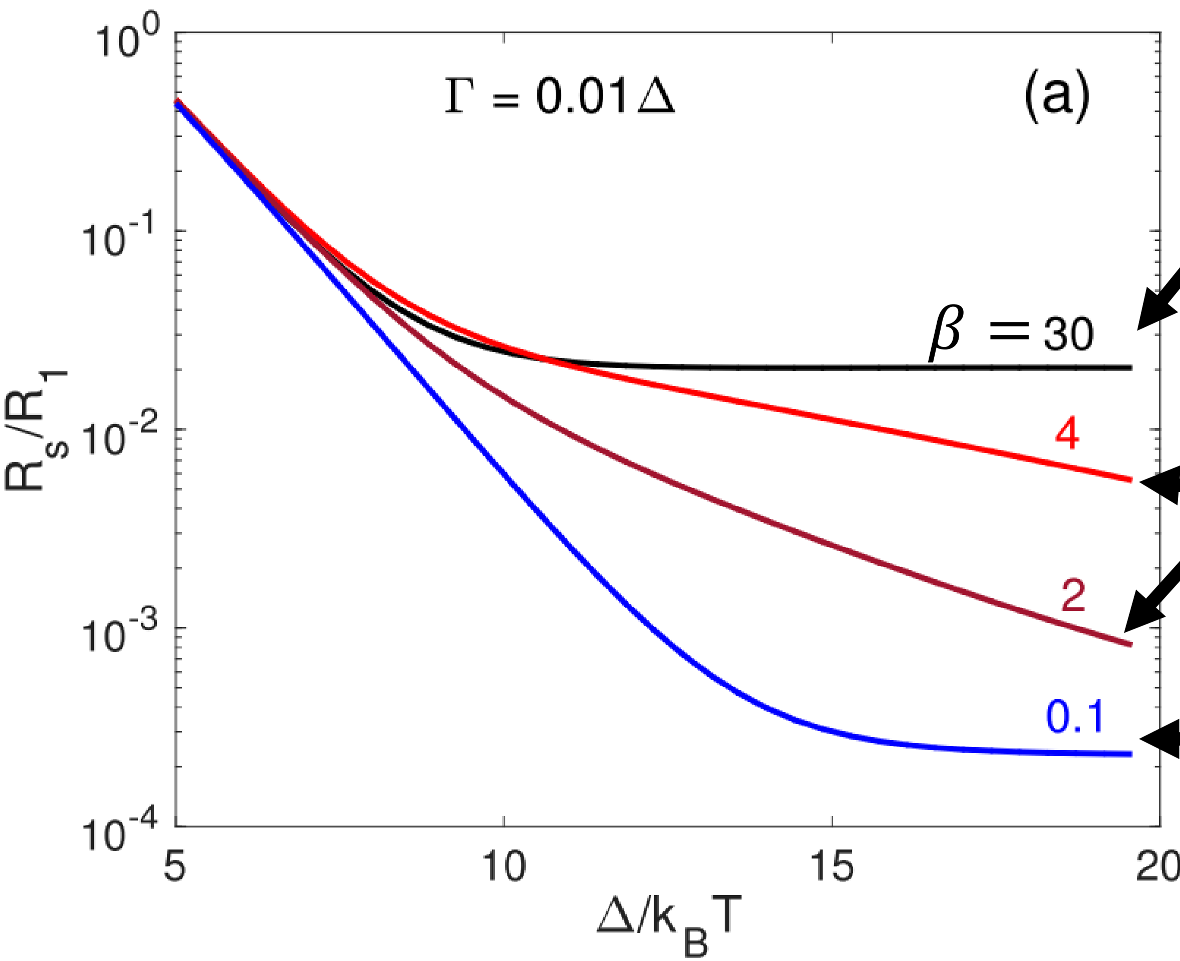

N and S are decoupled. The residual resistance is given by normal N.

The slope is changed to that corresponding to the minigap

Similar as the ideal surface with subgap states

FIG. 10. Arrhenius plots calculated from Eqs. (79)-(81) for $\alpha = 0.05$, $\lambda = 4\xi_S$, $\hbar\Omega = 11\Delta$, $D_n = D_s/3$, $\beta = 0.1,\ 2,\ 4,\ 30$, and (a) $\Gamma = 0.01\Delta$, (b) $\Gamma = 0.05\Delta$. Here $R_1 = \mu_0^2\omega^2\xi_S\lambda^2/2\rho_s$.

R_s as functions of T^{-1}

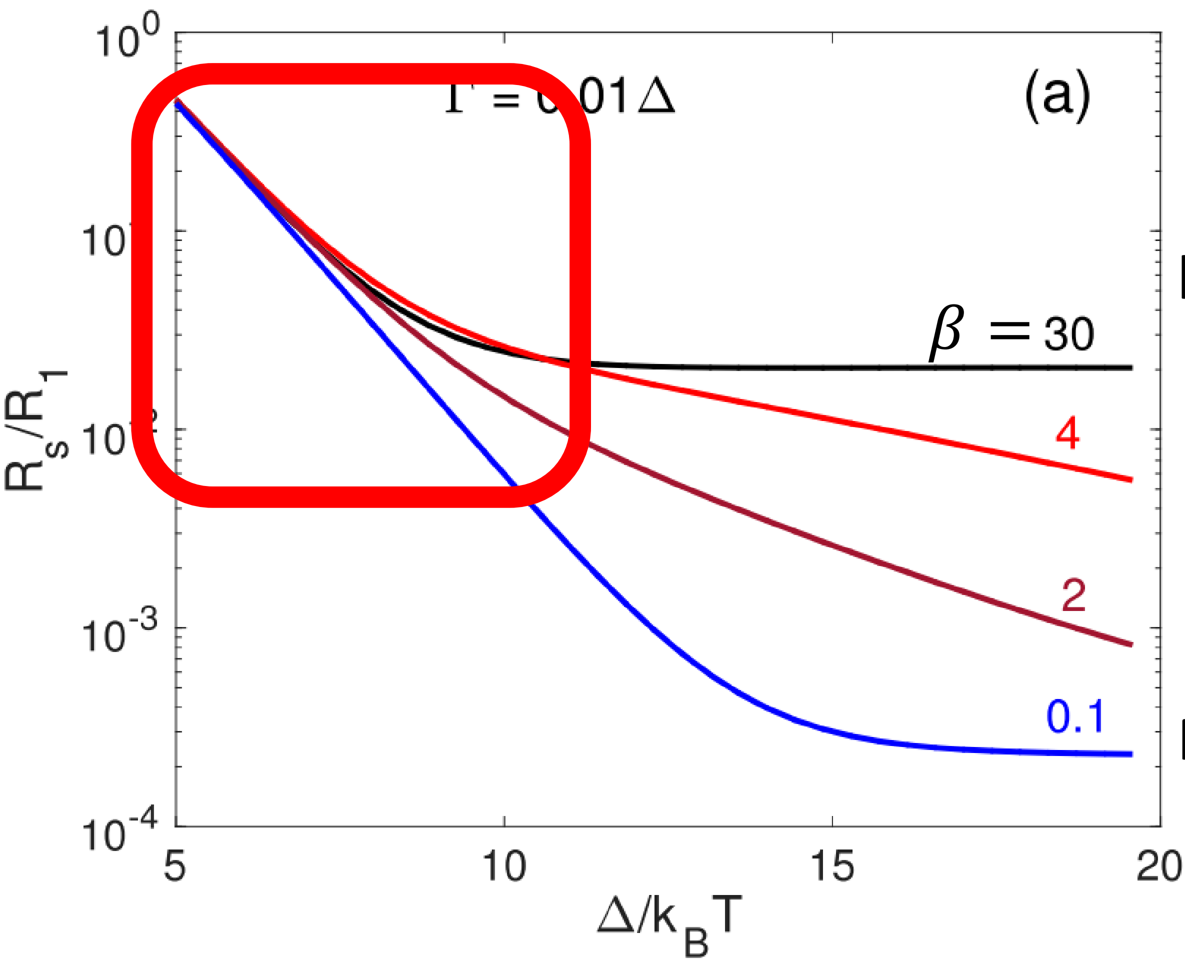

FIG. 10. Arrhenius plots calculated from Eqs. (79)-(81) for $\alpha = 0.05$, $\lambda = 4\xi_S$, $\hbar\Omega = 11\Delta$, $D_n = D_s/3$, $\beta = 0.1,\ 2,\ 4,\ 30$, and (a) $\Gamma = 0.01\Delta$, (b) $\Gamma = 0.05\Delta$. Here $R_1 = \mu_0^2\omega^2\xi_S\lambda^2/2\rho_s$.

Extrapolating the results obtained in a limited temperature window may lead to a wrong conclusion.

e.g. At Δ/kT < 10, the curves for β=4 and 30 are nearly the same: the traditional fitting based on $R_s=R_{MB}+R_i$ would suggest Ri at β=30, while their actual T dependence are much different at a lower T.

R_s as functions of T^{-1}

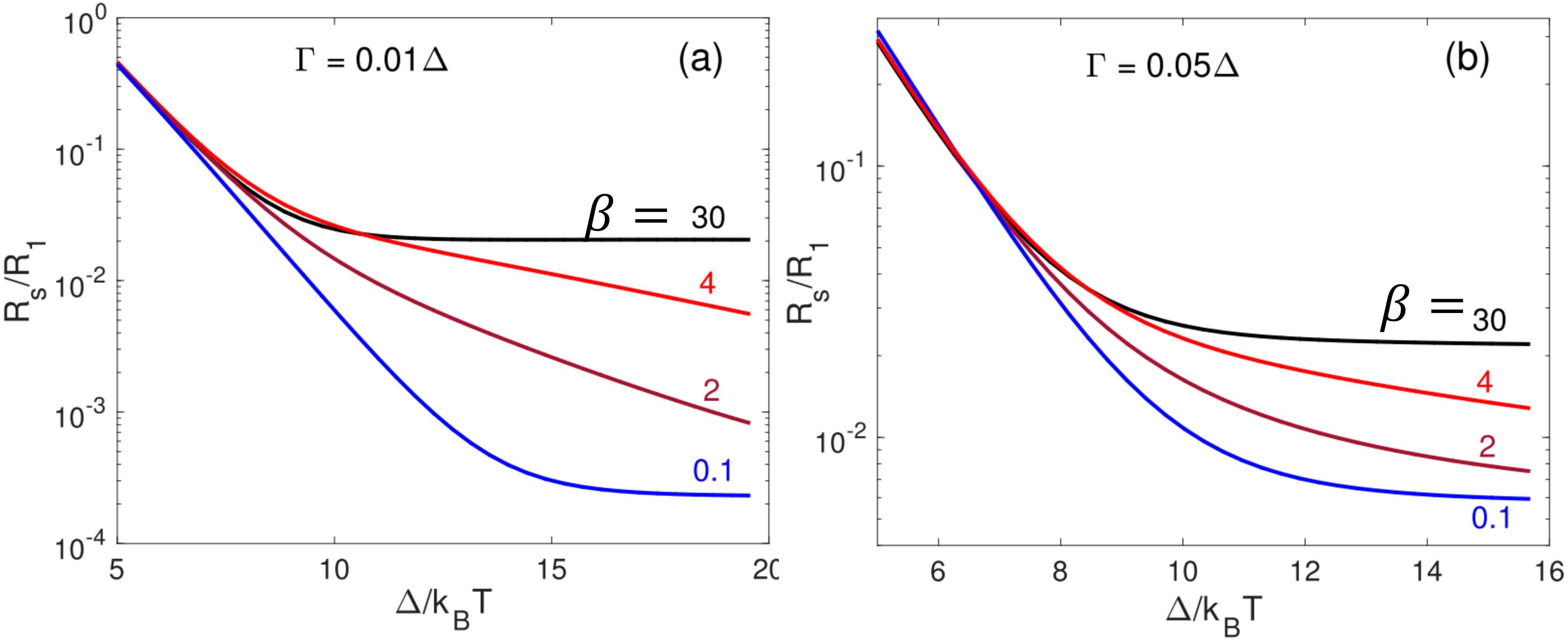

FIG. 10. Arrhenius plots calculated from Eqs. (79)-(81) for $\alpha = 0.05$, $\lambda = 4\xi_S$, $\hbar\Omega = 11\Delta$, $D_n = D_s/3$, $\beta = 0.1,\ 2,\ 4,\ 30$, and (a) $\Gamma = 0.01\Delta$, (b) $\Gamma = 0.05\Delta$. Here $R_1 = \mu_0^2\omega^2\xi_S\lambda^2/2\rho_s$.

R_s as functions of β for different T

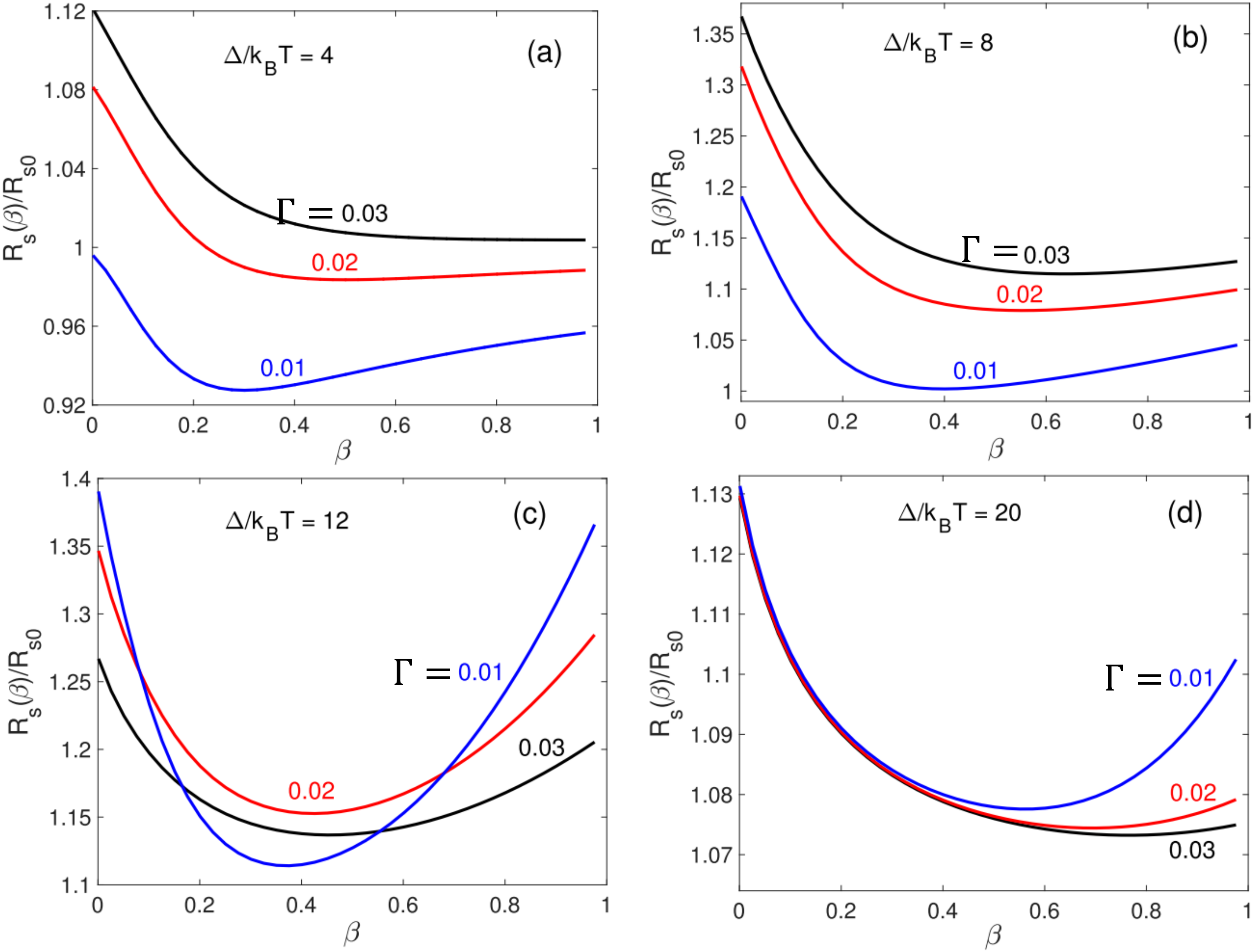

The minimum in Rs(β) mainly results from interplay of two effects.

The first effect which causes Rs to increase with β is rather transparent: as the barrier parameter β increases the proximity-induced superconductivity in N layer weakens, so the RF dissipation and Rs increase.

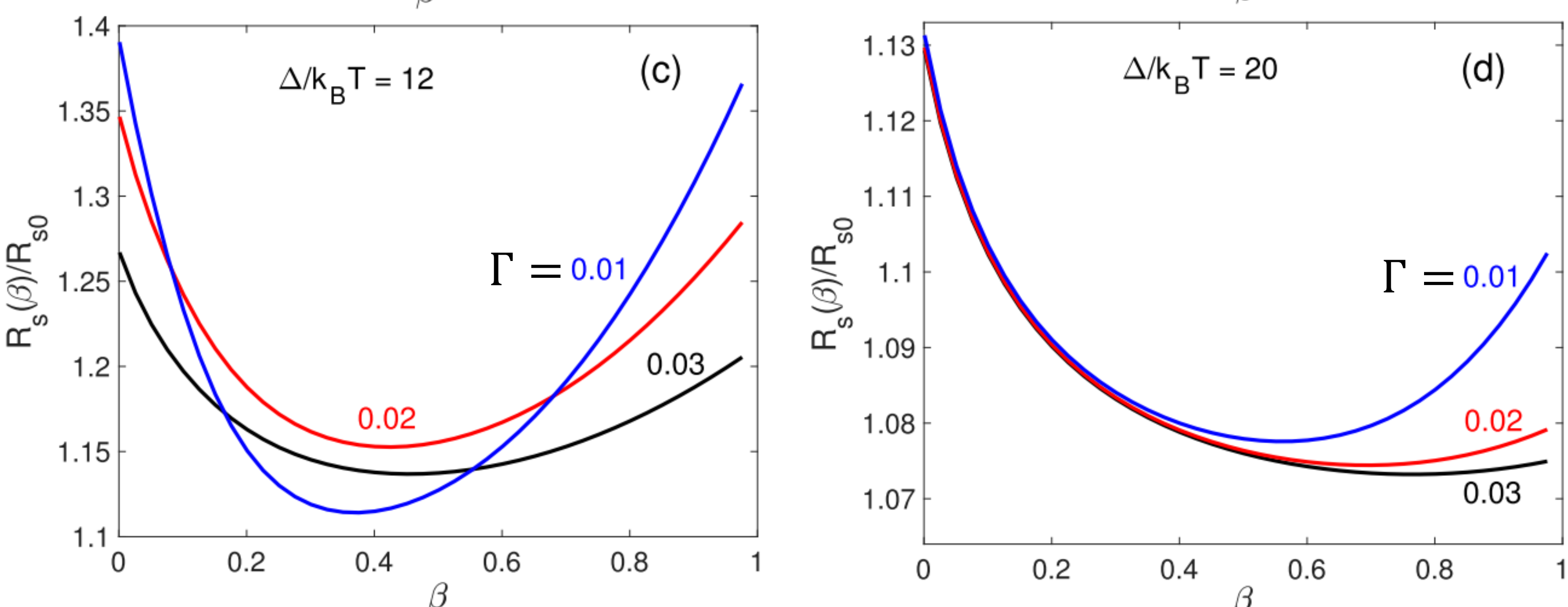

The minimum in Rs(β) mainly results from interplay of two effects.

<u>The first effect</u> which causes Rs to increase with β is rather transparent: as the barrier parameter β increases the proximity-induced superconductivity in N layer weakens, so the RF dissipation and Rs increase.

<u>The second effect</u> which causes the initial decrease of Rs with β results from the change in DOS around N layer. A moderate broadening of the gap peaks in N(ε) eliminates the BCS logarithmic divergence at ω→0 and reduces Rs .

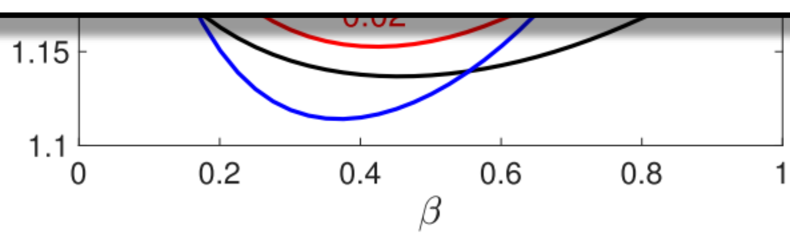

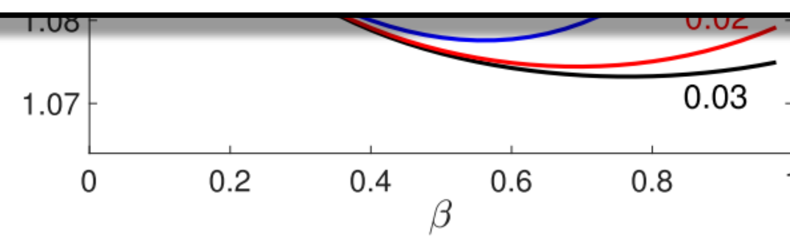

R_s as functions of β for different T

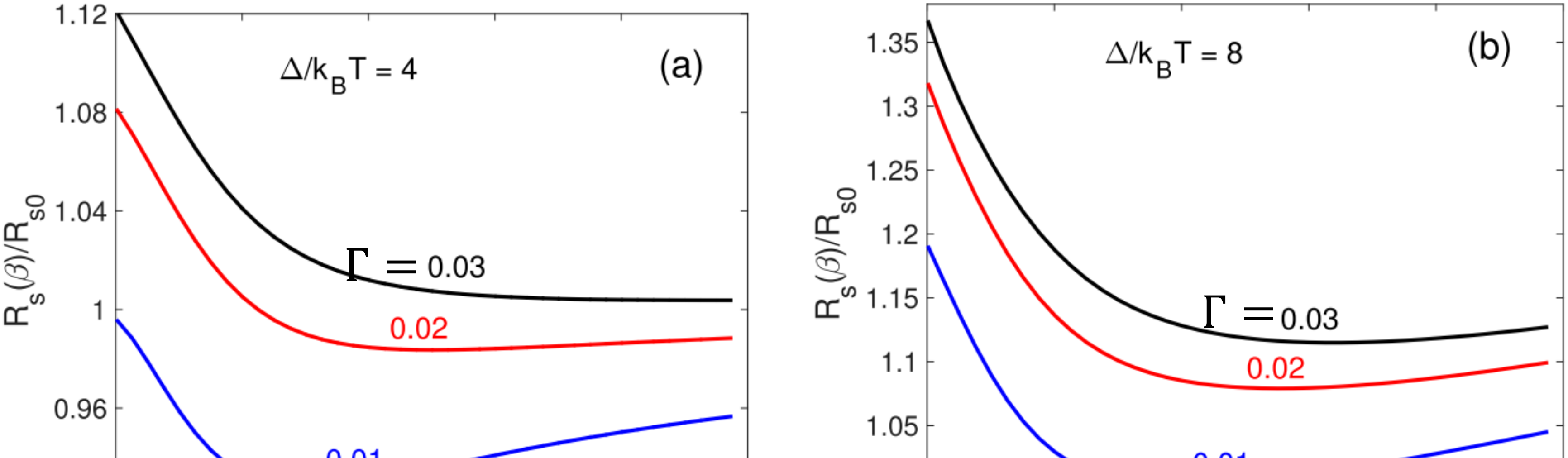

For Γ(<<Δ), optimum β is **β=0.2 – 1**.

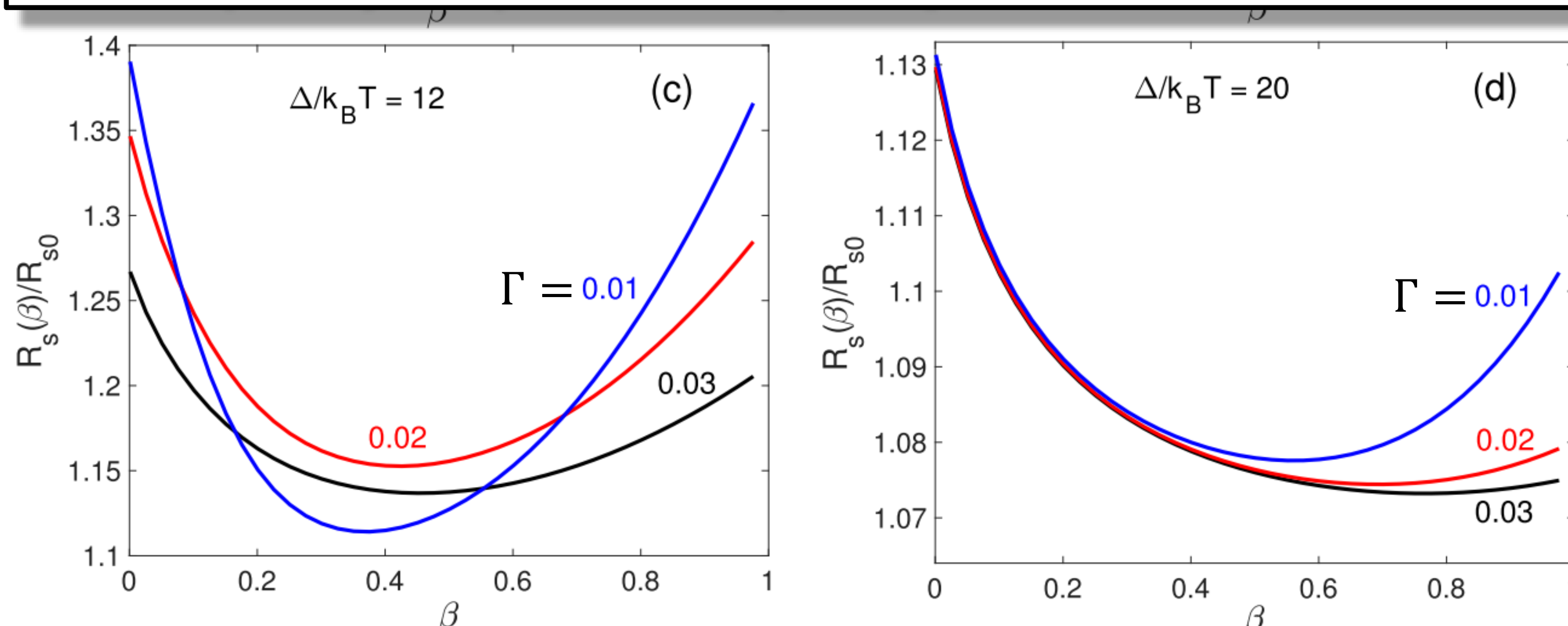

R_s as functions of β for different T

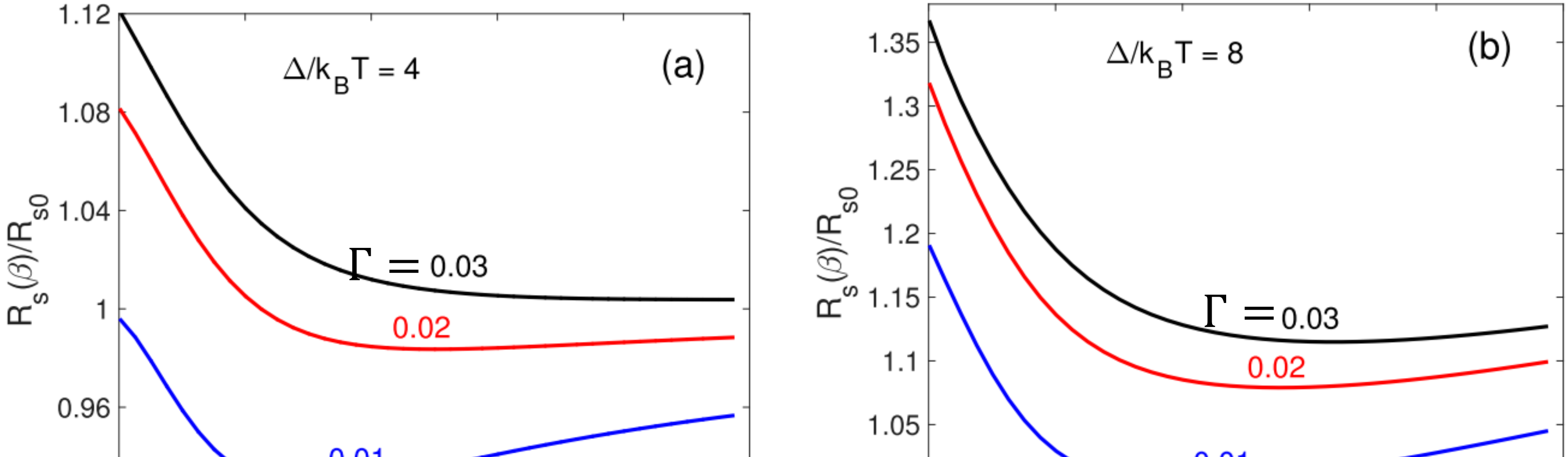

For Γ(<<Δ), optimum β is **β=0.2 – 1**.

Taking d=1nm, **β<1 corresponds to $R_B < 1.8*10^{-14}\Omega m^2$**

This is two orders of magnitude smaller than the lowest contact resistance of YBCO/Ag

[J. W. Ekin et al., Appl. Phys. Lett. **62**, 369 (1993)]

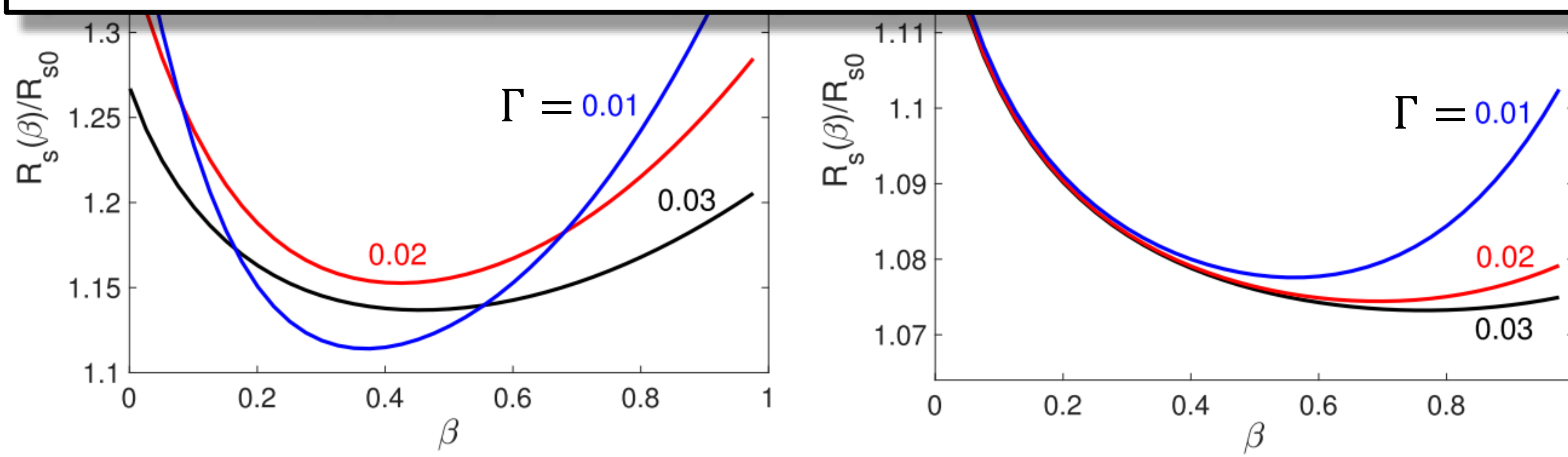

Surface Resistance

Bulk magnetic impurities

We will see broadening of DOS peak due to magnetic impurities can also reduce R_s.

We use the quasiclassical theory in the diffusive limit (Usadel eq.).

$$\epsilon \sinh\theta + i\Gamma_p \cosh\theta \sinh\theta = \tilde{\Delta}\cosh\theta$$

$$G^R = \cosh\theta \qquad F^R = \sinh\theta$$

$$\tilde{\Delta} = \Delta - \frac{\pi}{4}\Gamma_p, \qquad \Gamma_p \ll \Delta$$

$$\Gamma_p = \frac{\hbar v_F}{2\ell_p}$$

ℓ_p : mean spacing of magnetic impurities

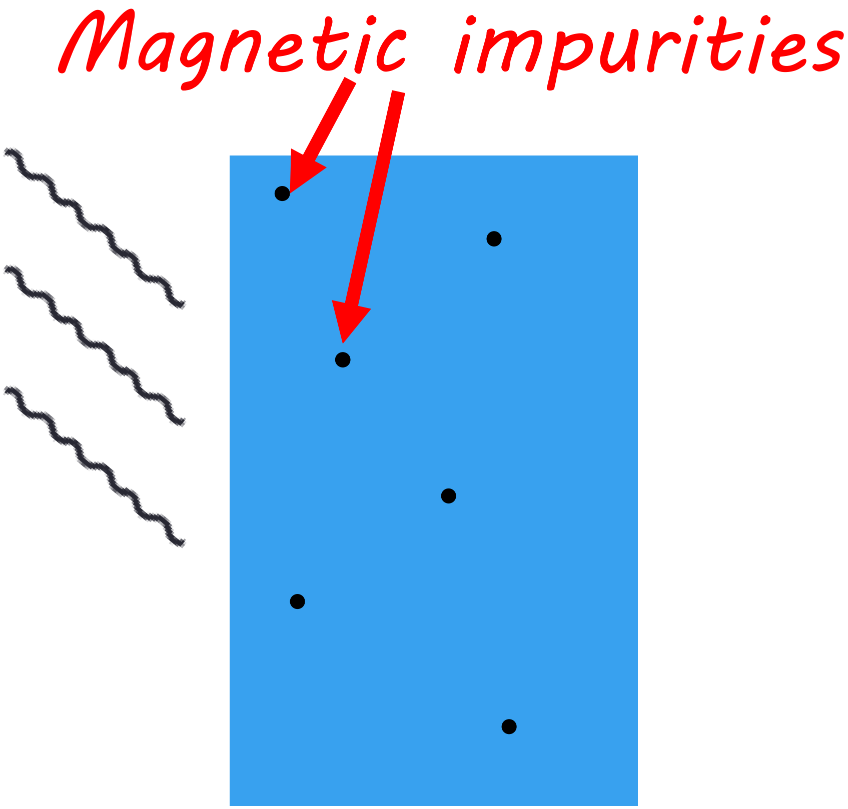

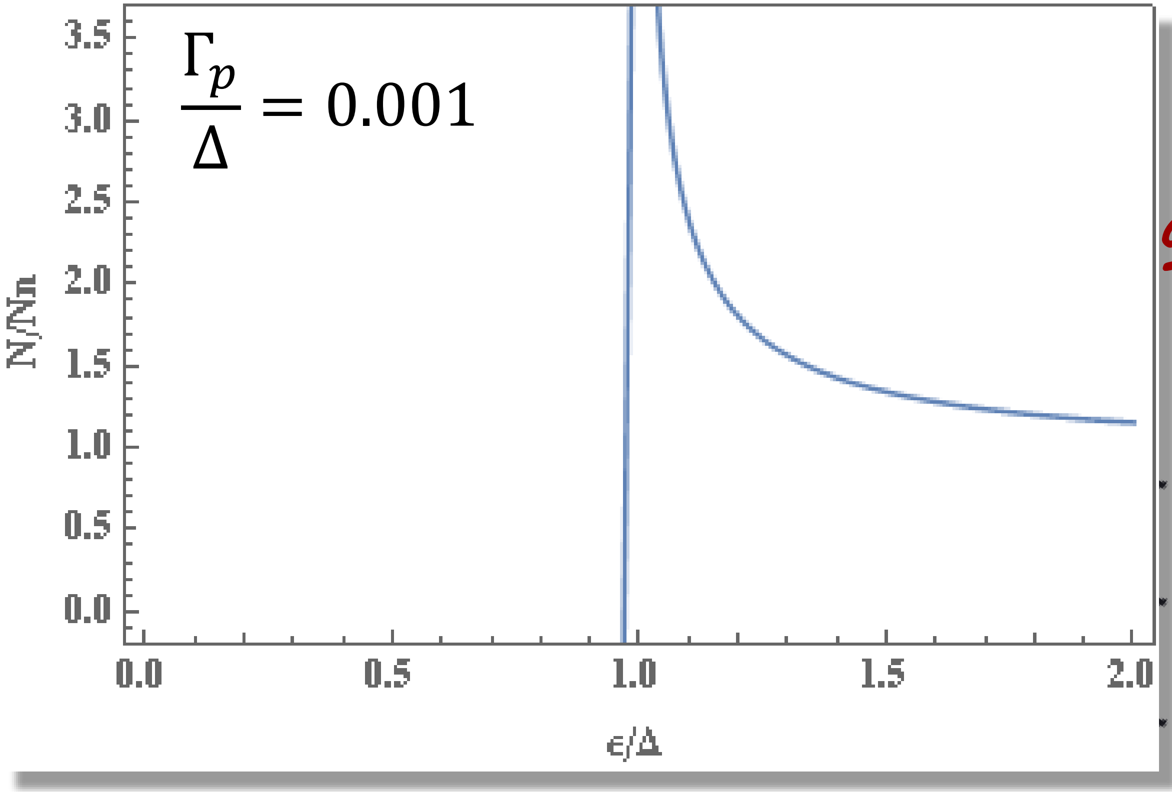

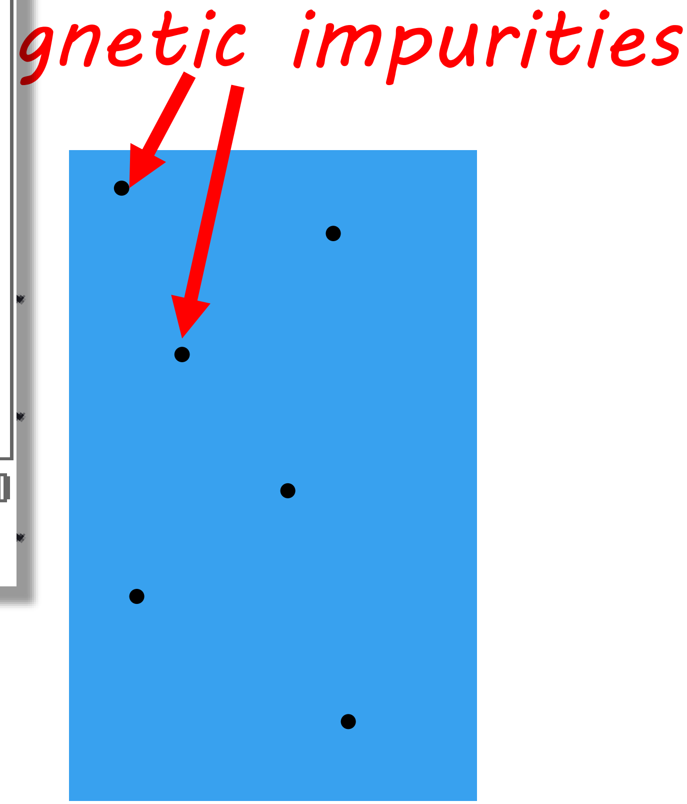

$$\Gamma_p = \frac{\hbar v_F}{2\ell_p}$$

ℓ_p : mean spacing of magnetic impurities

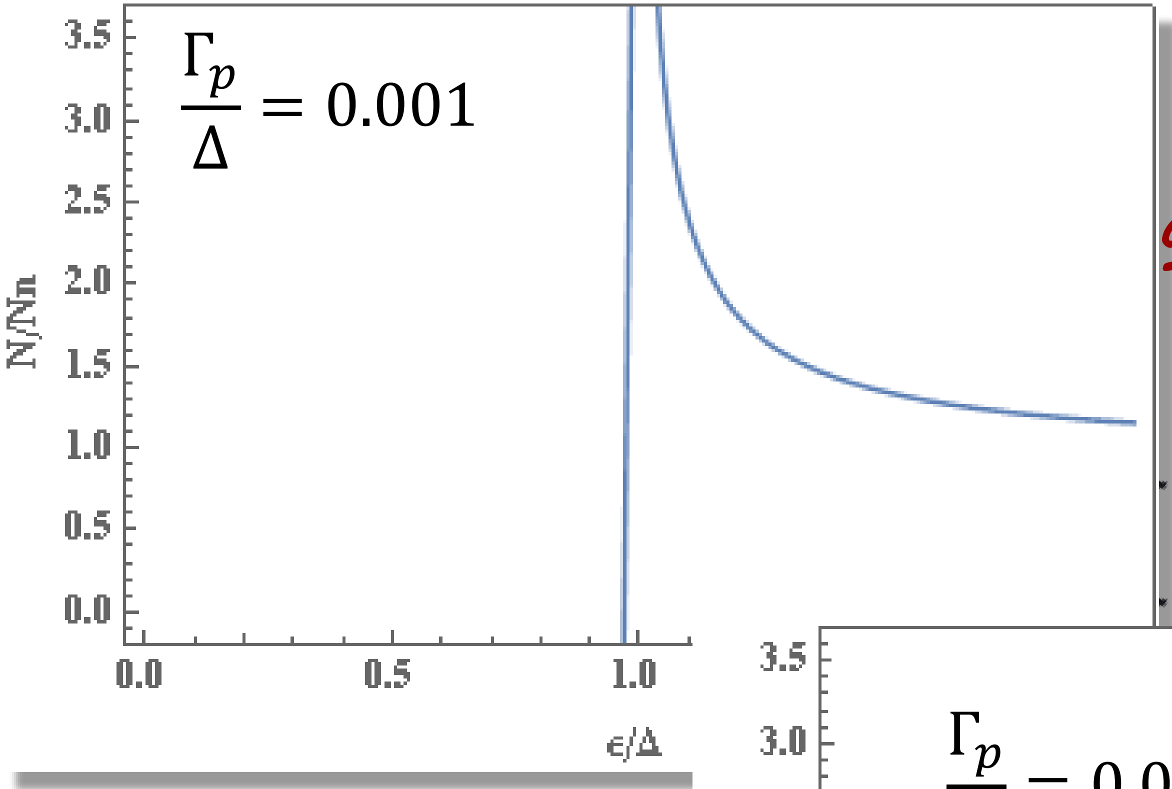

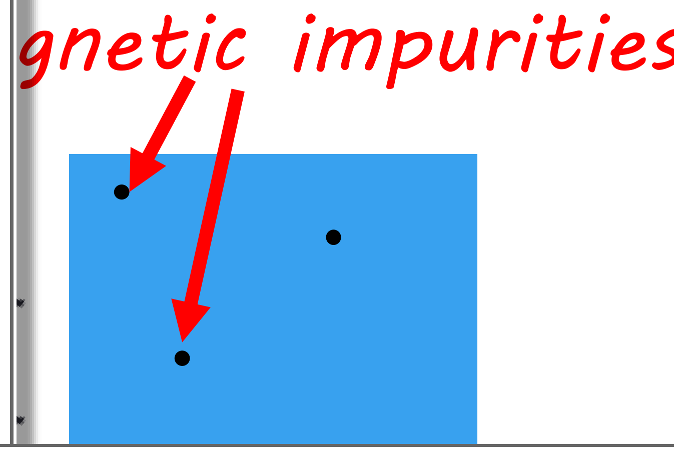

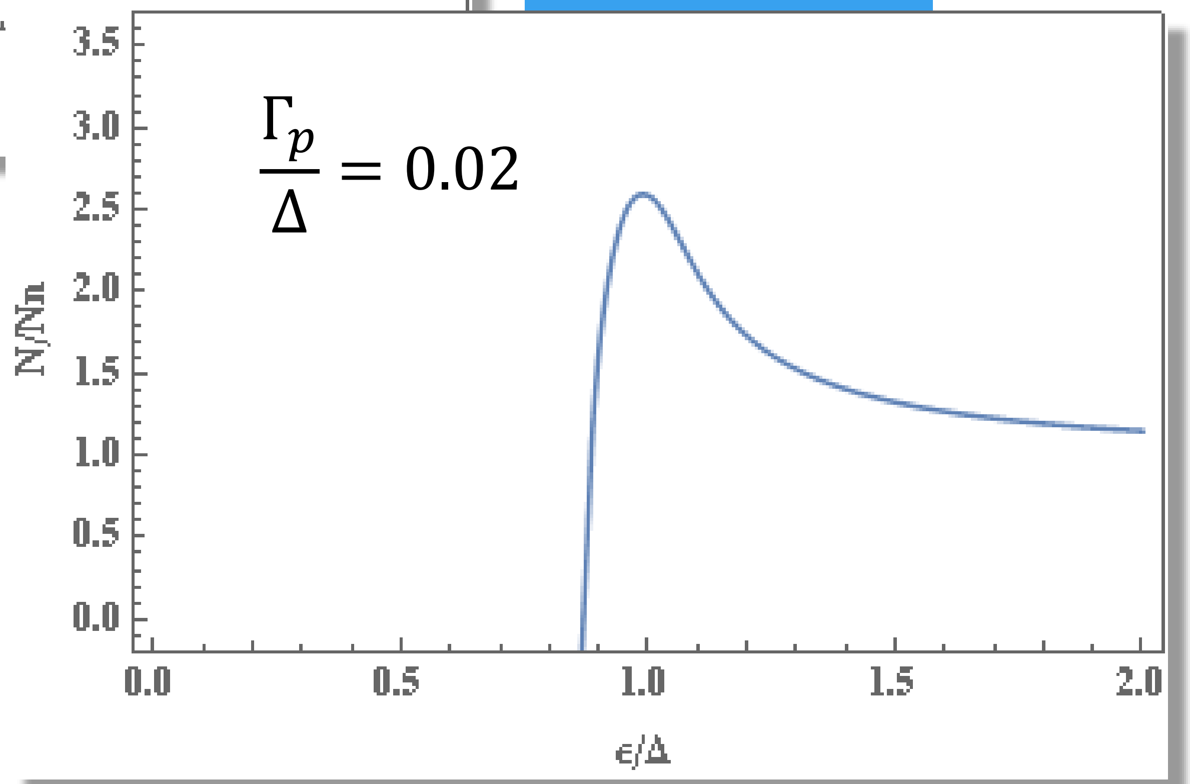

$$\Gamma_p = \frac{\hbar v_F}{2\ell_p}$$

ℓ_p : mean spacing of magnetic impurities

The surface resistance can be reduced by an appropriate density of magnetic impurities!

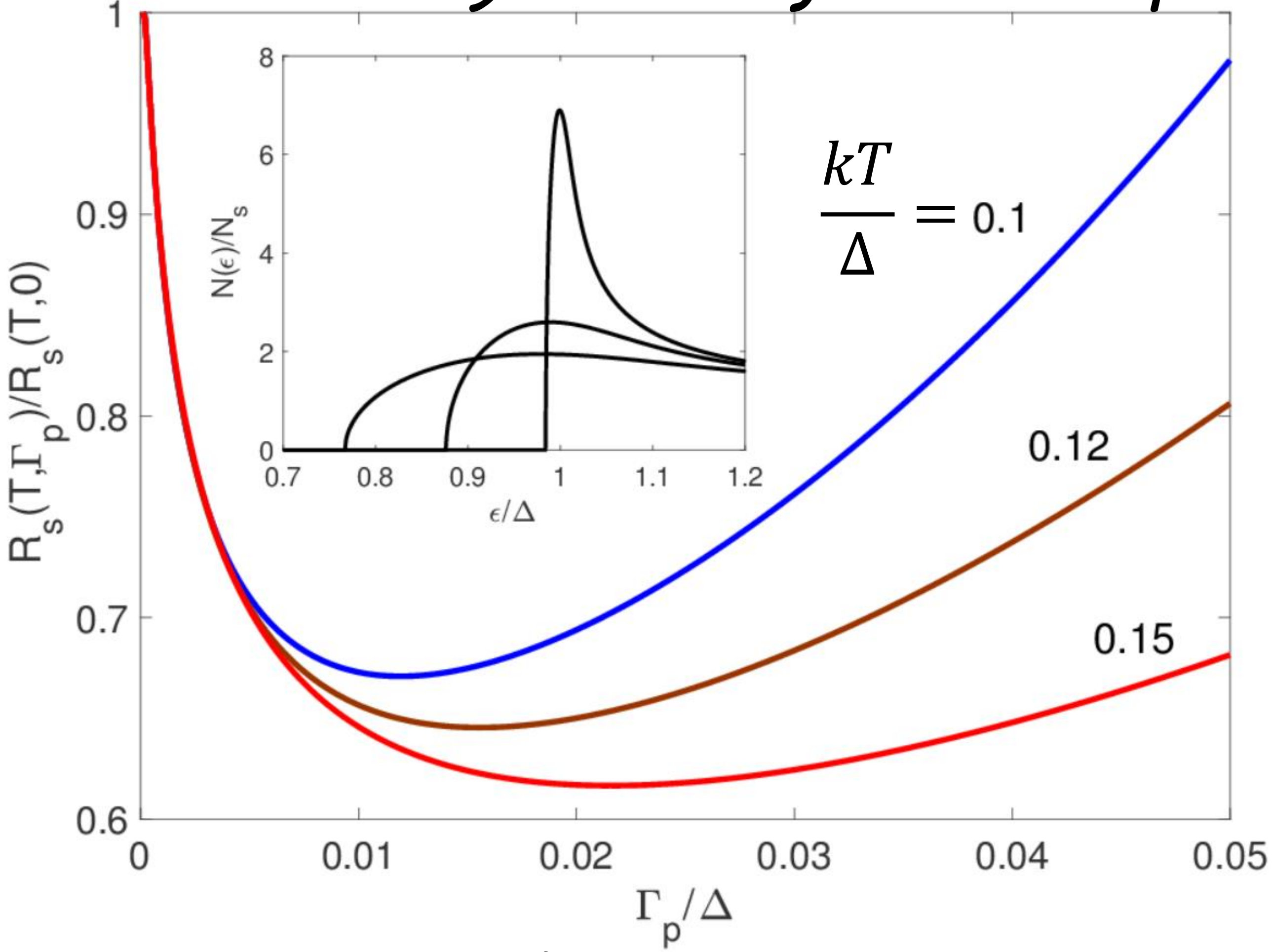

$\frac{\Gamma_p}{\Delta} \sim 0.01$ corresponds to the mean spacing of magnetic impurities $\ell_p \sim \frac{\xi_0}{0.01} \sim$ 4μm

Summary

Summary

- The main broadening effect can occur in a layer much thinner than λ: DOS in the bulk can be much sharper than the surface.
- Tunneling surface probes such as STM do not give all information about DOS in $x \lesssim \lambda$.
- Fitting the tunneling data of DOS with Dynes formula and extracting Γ to describe the low-T surface impedance Z can be misleading. A combination of tunneling measurement and Z in a sufficiently broad T range may offer a possibility to separate the surface and bulk contributions.

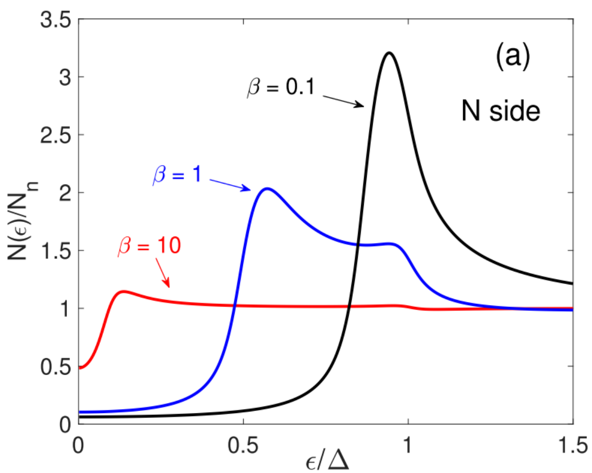

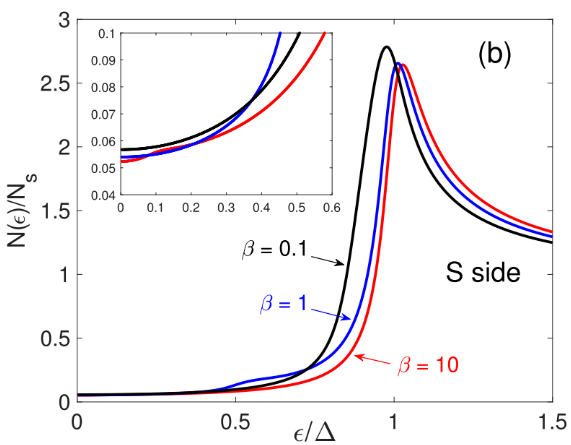

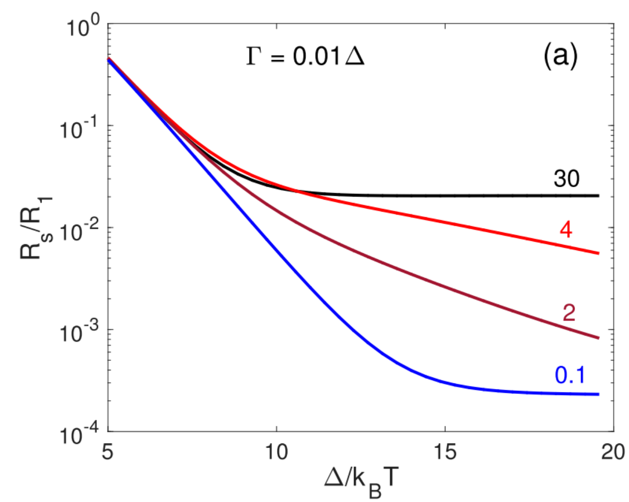

Summary (cont.)

- A thin pairbreaking layer or a weakly-coupled normal layer at the surface can radically (by orders of magnitude) increase R_i as compared to an ideal surface with only bulk broadening mechanisms.
- However, $R_s(T)$ can be reduced by optimizing DOS at the surface by tuning the properties of a proximity-coupled N layer at the surface. [$\beta<1$ corresponds to $R_B < 1.8*10^{-14}\Omega m^2$ for Nb with d=1nm normal layer]

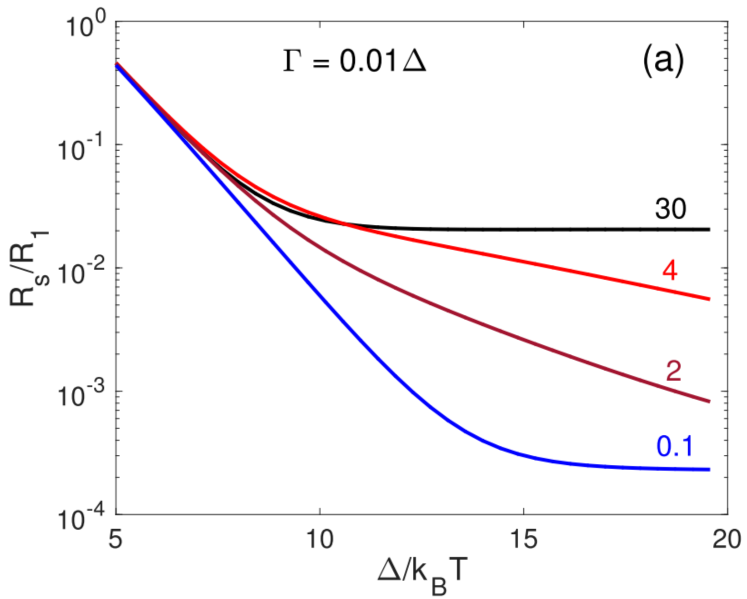

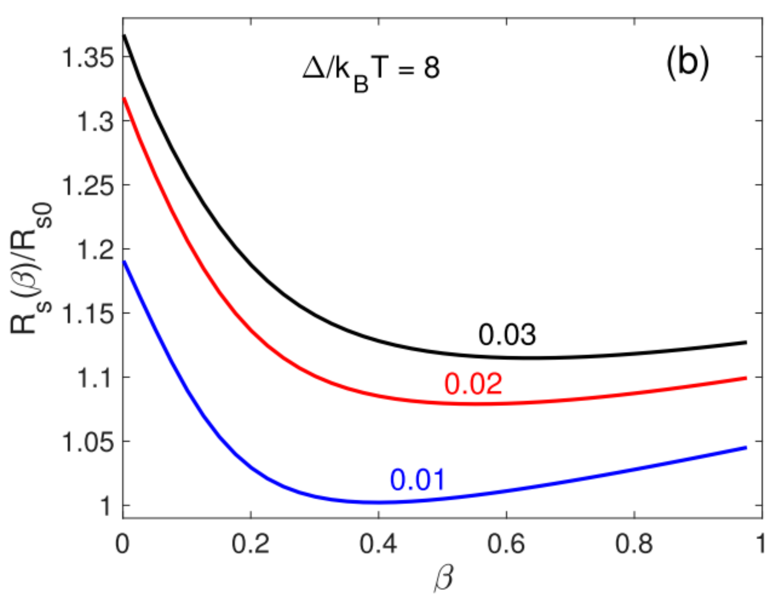

Summary (cont.)

- Introducing a tiny density of magnetic impurities ($\ell_p \sim \mu m$ for Nb) leads to moderator broaden DOS and reduces Rs.

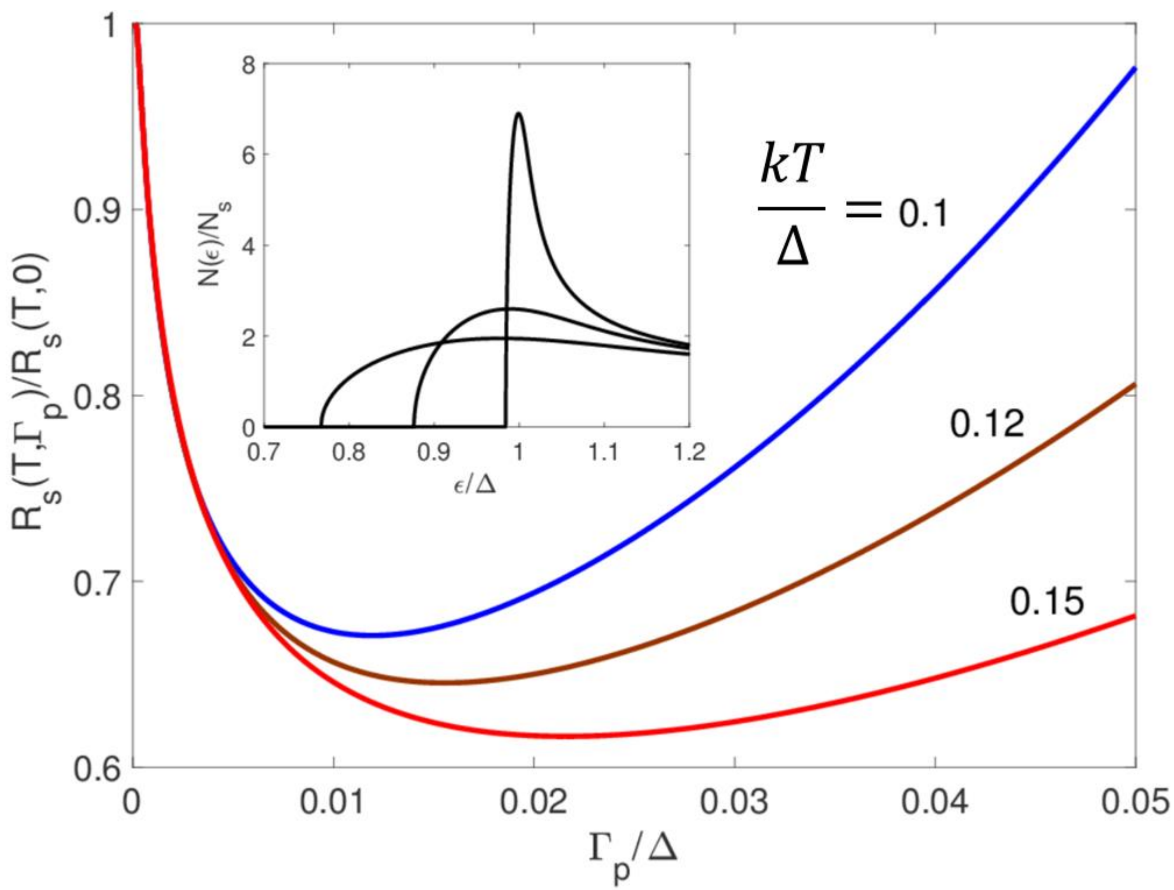

Backup
Units of temperature and surface resistance for Nb case

$$\frac{k_B T}{\Delta} \approx \frac{T}{17.5\mathrm{K}}$$

$$R_1 = \frac{\mu_0^2 \lambda^3 \omega \Delta}{2\hbar \rho_s} \sim 10^{-4}\Omega$$ (Slide 48)

$$R_1 = \frac{\mu_0^2 \omega^2 \lambda^2 \xi_s}{2\rho_s} \sim 10^{-7}\Omega$$ (Slide 59)